

**Title:** Endogenous CD28 drives CAR T cell responses in multiple myeloma

**Author List and Affiliations:** Mackenzie M. Lieberman<sup>1</sup>, Jason H. Tong<sup>1</sup>, Nkechi U. Odukwe<sup>1</sup>, Colin A. Chavel<sup>1</sup>, Terence J. Purdon<sup>2</sup>, Rebecca Burchett<sup>3</sup>, Bryan M. Gillard<sup>4</sup>, Craig M. Brackett<sup>5</sup>, A. J. Robert McGray<sup>1</sup>, Jonathan L. Bramson<sup>3</sup>, Renier J. Brentjens<sup>1,2</sup>, Kelvin P. Lee<sup>6</sup>, Scott H. Olejniczak<sup>1\*</sup>

<sup>1</sup>Department of Immunology, Roswell Park Comprehensive Cancer Center, Buffalo, NY 14263, USA.

<sup>2</sup>Department of Medicine, Roswell Park Comprehensive Cancer Center, Buffalo, NY 14263, USA.

<sup>3</sup>Department of Pathology and Molecular Medicine, McMaster Immunology Research Centre, McMaster University, Hamilton, ON, Canada.

<sup>4</sup>Department of Pharmacology and Therapeutics, Roswell Park Comprehensive Cancer Center, Buffalo, NY, USA.

<sup>5</sup>Department of Cell Stress Biology, Roswell Park Comprehensive Cancer Center, Buffalo, NY 14263, USA.

<sup>6</sup>Indiana University Melvin and Bren Simon Comprehensive Cancer Center, Indianapolis, IN, 46202, USA.

\*Corresponding author: Scott H. Olejniczak, Department of Immunology, Roswell Park Comprehensive Cancer Center, Carlton and Elm Streets, Buffalo, NY 14203. Phone: 716-845-8538; Email: [scott.olejniczak@roswellpark.org](mailto:scott.olejniczak@roswellpark.org)

1    **Abstract**

2       Recent FDA approvals of chimeric antigen receptor (CAR) T cell therapy for multiple  
3 myeloma (MM) have reshaped the therapeutic landscape for this incurable cancer. In pivotal  
4 clinical trials B cell maturation antigen (BCMA) targeted, 4-1BB co-stimulated (BBζ) CAR T cells  
5 dramatically outperformed standard-of-care chemotherapy, yet most patients experienced MM  
6 relapse within two years of therapy, underscoring the need to improve CAR T cell efficacy in  
7 MM. We set out to determine if inhibition of MM bone marrow microenvironment (BME) survival  
8 signaling could increase sensitivity to CAR T cells. In contrast to expectations, blocking the  
9 CD28 MM survival signal with abatacept (CTLA4-Ig) accelerated disease relapse following CAR  
10 T therapy in preclinical models, potentially due to blocking CD28 signaling in CAR T cells.  
11 Knockout studies confirmed that endogenous CD28 expressed on BBζ CAR T cells drove *in*  
12 *vivo* anti-MM activity. Mechanistically, CD28 reprogrammed mitochondrial metabolism to  
13 maintain redox balance and CAR T cell proliferation in the MM BME. Transient CD28 inhibition  
14 with abatacept restrained rapid BBζ CAR T cell expansion and limited inflammatory cytokines in  
15 the MM BME without significantly affecting long-term survival of treated mice. Overall, data  
16 directly demonstrate a need for CD28 signaling for sustained *in vivo* function of CAR T cells and  
17 indicate that transient CD28 blockade could reduce cytokine release and associated toxicities.

18

19    **Keywords:** CD28, co-stimulation, CAR T cells, multiple myeloma, tumor microenvironment,  
20 metabolism

21

22

23

## 24 **Introduction**

25 Chimeric Antigen Receptor (CAR) T cells are a form of immunotherapy that has seen  
26 extraordinarily success in treating hematologic malignancies<sup>1-12</sup>. Expression of a CAR in  
27 autologous T cells isolated from cancer patients redirects T cell specificity toward an antigen of  
28 interest and delivers activation signals upon antigen ligation<sup>13-15</sup>. Activation signals in clinically  
29 relevant second-generation CAR T cells are mediated by CD3 $\zeta$  as well as a co-stimulatory  
30 domain, most commonly CD28 or 4-1BB, although others including ICOS and OX40 remain  
31 under investigation<sup>16-21</sup>. Second generation CAR T cells targeting the B cell antigen, CD19, are  
32 FDA approved for B cell leukemias and lymphomas and have resulted in potent, decade long  
33 remissions for some of the initial patients who received this therapy<sup>7,10,22-24</sup>. Within the last few  
34 years, FDA approval for CAR T cells has expanded to include those directed against the tumor  
35 necrosis factor receptor (TNF-R) superfamily molecule, B cell maturation antigen (BCMA) for  
36 the treatment of multiple myeloma (MM)<sup>25,26</sup>. Despite robust initial response rates greatly  
37 outperforming standard of care in heavily pre-treated MM patient populations, recent clinical  
38 studies have shown that approximately 40% of MM patients will experience disease progression  
39 within the first 24 months of BCMA-targeted CAR T cell infusion<sup>27-29</sup>. Therefore, there is an  
40 urgent need to understand and overcome resistance mechanisms that hinder CAR T cell  
41 success in MM patients.

42 MM remains an incurable malignancy of plasma cells, a terminally differentiated B cell  
43 subset that typically reside in the bone marrow (BM) and contribute to protective humoral  
44 immunity through the production of immunoglobulin. The long-term survival of plasma cells is  
45 critically dependent upon interactions occurring within the BM niche, with many soluble and  
46 contact-dependent stromal interactions also contributing to survival and disease progression of  
47 MM<sup>30</sup>. MM relies on CXCL12 chemokine gradients to home into the BM niche, as well as  
48 adhesion molecules including LFA-1 to mediate attachment and retention within the  
49 microvasculature<sup>31-34</sup>. Several soluble mediators secreted by BM resident dendritic cells (DCs),

50 macrophages, osteoblasts, and stromal cells, including IL-6 and BCMA ligands, APRIL, and  
51 BAFF, sustain MM survival and proliferation<sup>35-40</sup>. Additionally contact-dependent interactions  
52 regulate anti-apoptotic molecule expression and chemotherapeutic resistance in MM. A key  
53 mediator of contact-dependent survival in MM is the canonical T cell co-stimulatory receptor,  
54 CD28, whose expression on MM cells is highly correlated with myeloma progression<sup>41</sup>.  
55 Importantly, CD28 ligands CD80 and CD86 are expressed on DCs, stromal cells, and even  
56 MM cells within the BM microenvironment<sup>30,42-44</sup>. Ligation of CD28 on MM cells by CD80/CD86  
57 transduces a PI3K/Akt pathway dependent, pro-survival signal protecting them from  
58 chemotherapy and growth factor withdrawal-induced death<sup>42,45-47</sup>. Importantly, CD28 interaction  
59 with CD80/CD86 can be blocked by the CTLA4-Ig fusion protein abatacept, which is FDA  
60 approved for the treatment of rheumatoid arthritis, psoriatic arthritis, polyarticular juvenile  
61 idiopathic arthritis and acute graft versus host disease<sup>48,49</sup>. In myeloma, pre-clinical studies have  
62 shown that CTLA4-Ig in combination with melphalan can significantly reduce tumor burden<sup>45</sup>,  
63 leading to a phase II clinical trial of abatacept plus standard of care chemotherapy for treatment  
64 of patients with relapsed/refractory MM (NCT03457142).

65 Given the recently reported ~3-fold improvement in overall response rate when abatacept  
66 was added to standard of care therapy<sup>50</sup>, we hypothesized that systemic blockade of CD28  
67 would similarly sensitize MM to CAR T cell therapy. We reasoned that unlike endogenous T cells  
68 that require CD28 co-stimulation to mount an anti-tumor response, second generation CAR T  
69 cells receive co-stimulation directly from the CAR and would therefore be relatively unaffected  
70 by blockade of endogenous CD28. FDA approved CAR T cell products for MM, idacabtagene  
71 vicleucel and ciltacabtagene autoleucel, employ 4-1BB co-stimulatory domains, which have  
72 been shown to transduce a weaker signal than CD28 co-stimulatory domains in CD19 targeted  
73 CAR T cells<sup>51,52</sup>. In this context, the weaker 4-1BB co-stimulatory signal reduced CAR T cell  
74 exhaustion and enhanced *in vivo* persistence when compared to CD28 driven co-  
75 stimulation<sup>53,54</sup>. However, recent evidence suggests that enhanced CD28 signaling in CTLA-4

76 knockout 4-1BB co-stimulated (BBζ) CAR T cells improves their anti-tumor efficacy<sup>55</sup>. Moreover,  
77 endogenous tumor-reactive cytotoxic T cells require CD28 signaling to acquire effector  
78 properties in the tumor microenvironment<sup>56</sup>, suggesting that perhaps the CAR 4-1BB co-  
79 stimulatory domain alone is insufficient to stimulate potent anti-tumor activity.

80 In the current study, we employed human and mouse orthotopic models of multiple myeloma  
81 (MM) to directly test whether endogenous CD28 affected tumor control by BCMA targeted, 4-  
82 1BB co-stimulated CAR T cells. Somewhat unexpectedly, we found that continuous blockade of  
83 CD28 interaction with B7 proteins using abatacept significantly impaired CAR T cell control of  
84 MM growth, resulting in shorter survival of MM-bearing mice. Data indicate that abatacept  
85 primarily affected endogenous CD28 signaling on CAR T cells, as inducible deletion of CD28  
86 from 4-1BB co-stimulated CAR T cells also reduced their *in vivo* anti-MM efficacy.  
87 Mechanistically, we provide evidence that endogenous CD28 signaling increases 4-1BB co-  
88 stimulated CAR T cell expansion in the MM bone marrow microenvironment (BME) by  
89 stimulating oxidative phosphorylation and maintaining redox balance. Transient inhibition of  
90 endogenous CD28 on 4-1BB co-stimulated CAR T cells resulted in decreased accumulation of  
91 CD4<sup>+</sup> CAR T cells and release of inflammatory cytokines in the MM TME, without significantly  
92 impairing anti-MM activity. Collectively, our findings reveal that CAR T cell function is affected by  
93 endogenous CD28, which can potentially be transiently blocked to reduce toxic pro-  
94 inflammatory cytokine release while maintaining anti-tumor activity.

95

## 96 **Materials and Methods**

97 *Cell lines:* Parental 5TGM1 cells generously provided by G. David Roodman (Indiana University)  
98 were lentivirally transduced to express truncated human BCMA (hBCMA) and firefly luciferase to  
99 be used as target cells. Pure populations were achieved following fluorescence-activated cell  
100 sorting. MM.1S and U266 luciferase expressing clones were generated and supplied by Kelvin  
101 Lee (Indiana University). MM cell lines were maintained in RPMI 1640 (Gibco) supplemented

102 with 10% heat-inactivated FBS (R&D Systems), 1% nonessential amino acids (Gibco), 1mM  
103 sodium pyruvate (Gibco), 10 mM HEPES (Gibco), 2 mM L-glutamine (Gibco) and 1%  
104 penicillin/streptomycin (Gibco). Cell lines were maintained in culture for 2-3 months at a time.  
105 293T packaging cell lines were purchased from ATCC and maintained in DMEM, 10% FBS and  
106 1% L-glutamine for 2-3 weeks prior to transient transfection. Stably expressing 293 Galv9 cells  
107 were kindly provided by Renier Brentjens. All cell lines were routinely tested for mycoplasma  
108 using the Lonza MycoAlert Detection Kit.

109

110 *Construct generation:* Second generation CAR constructs were generously provided by  
111 Jonathan Bramson (McMaster University) and Renier Brentjens (Roswell Park)<sup>57</sup>.

112 *Mouse ahBCMA CAR (hBCMA<sub>m</sub>BB<sub>m</sub>ζ)* : CAR encoding DNA was subcloned into the multiple  
113 cloning site of the pRV2011 retroviral vector which also contains an internal ribosome entry site  
114 (IRES) and Thy1.1. Murine CAR constructs consisted of an anti-human BCMA single chain  
115 variable fragment (scFv) (C11D5.3), CD8 hinge, CD28 transmembrane, 4-1BB signaling domain  
116 and CD3ζ activation domain as described previously<sup>58</sup>.

117 *Mouse ahCD19 CAR (hCD19<sub>m</sub>28<sub>m</sub>ζ)* : Off-target CAR constructs consisted of an anti-human  
118 CD19 scFv (FMC63), CD28 transmembrane, CD28 signaling domain and CD3ζ activation  
119 domain.

120 *Human ahBCMA CAR (hBCMABB<sub>h</sub>ζ)* : Antigen recognition was defined by an anti-human BCMA  
121 scFv previously reported. Human CAR constructs consisted of an CD8a hinge, CD8a  
122 transmembrane, CD28 or 4-1BB signaling domain and CD3ζ activation domain<sup>57,59</sup>.

123 *hBCMA-tNGFR:* Lentiviral expression plasmid, LeGO-Luc2, was a gift from Boris Fehse  
124 (Addgene plasmid #154006) which was further modified to co-express hBCMA-tNGFR. Murine  
125 5TGM1 cells were transduced with lentiviral supernatant to drive expression of the target  
126 antigen, hBCMA, and permit *in vivo* imaging of tumor bearing animals.

127 All constructs were verified by sanger sequencing.

128

129 *Mouse CAR T cell production:* Mouse CAR T cell production was adapted from previous reports  
130 <sup>60</sup>. Briefly, pan CD3<sup>+</sup> murine T cells were isolated from single cell splenocyte suspensions of 6 –  
131 12-week-old mice through a negative selection process (STEMCELL Technologies). T cells were  
132 activated with  $\alpha$ CD3/ $\alpha$ CD28 Dynabeads as specified by manufacturer's instructions in the  
133 presence of 100 IU/mL recombinant mouse (rm) IL-2 and 10 ng/mL rmlL-7 (BioLegend) and  
134 cultured in RPMI1640 supplemented with 10% FBS, 2 mM L-glutamine, 10mM HEPES, 0.5% 2-  
135 mercaptoethanol, and 1% penicillin/streptomycin. Retroviral transduction was achieved by  
136 spinoculation of  $3 \times 10^6$  mouse T cells on retronectin-coated plates (Takara Bio) with neat  
137 retroviral supernatant harvested from 293T packaging cells (2000xg, 60 min., 30 °C) at 24 and  
138 48 hr. post activation. CAR T cells were maintained at  $1 \times 10^6$  cells/mL for 7-10 days *in vitro* in  
139 the presence of rmlL-2 and rmlL-7 <sup>60</sup>.

140

141 *Human CAR T cell production:* Human CAR T cell production was adapted from previously  
142 published protocols <sup>57</sup>. De-identified, healthy donor peripheral blood mononuclear cells (PBMCs)  
143 were obtained through the Roswell Park donor center under the approved protocol BDR  
144 115919. PBMCs were isolated from whole blood through density gradient centrifugation. PBMCs  
145 were activated with T cell TransAct polymeric nanomatrix (Miltenyi Biotec) according to  
146 manufacturer's specifications in the presence of 100 IU/mL recombinant human (rh) IL-2 and 10  
147 ng/mL rhIL-7 (Peprotech). Spinoculation with neat 293 Galv9 retroviral supernatant was  
148 performed at 48, 72 and 96 hr. post activation (3200 rpm, 60 min., 30 °C). Human CAR T cells  
149 were expanded for 14 days and subsequently cryopreserved in 90% FBS, 10% DMSO.

150

151 *Cytotoxicity assays:* *In vitro* CAR T cell killing assays were performed using firefly luciferase  
152 expressing target cells. Briefly,  $2 \times 10^4$  target cells were seeded in 96 well plates, varying  
153 numbers of CAR T cells were added to assess CAR T cell mediated killing within the linear

154 range. Target cell viability following co-culture incubation was determined using the ONE-glo  
155 luciferase reporter assay (Promega). For cytokine secretion assays, supernatants were  
156 collected 24 hrs. after co-culture and analyzed on a Luminex xMAP INTELLIFLEX system.

157

158 *Flow cytometry:* Data was acquired on either a LSR Fortessa (BD Biosciences) or Cytex Aurora  
159 full spectrum analyzer (Cytex Biosciences). Analysis was performed using FlowJo (Tree Star  
160 Inc.) or FCS Express software (De novo Software). Briefly, cell suspensions were harvested,  
161 washed, and stained with fixable live/dead blue (Invitrogen) in PBS followed by surface antibody  
162 staining in FACS buffer (1% BSA, 0.1% sodium azide in PBS). Antibodies were titrated for  
163 optimal staining for 20 min. at 4°C. Intracellular cytokine staining was conducted following  
164 fixation and permeabilization according to manufacturer's instructions (BioLegend). Antibodies  
165 used in phenotypic analysis are included in Supplemental Table 1.

166

167 *Cytokine analyses (Luminex and Isoplexis):* Co-culture supernatants were immediately snap  
168 frozen and stored at -80 °C until Luminex assays were run. Detection of mouse CAR T cell  
169 cytokine production was performed using the MILLIPLEX Th17 premixed panel and acquired on  
170 a Luminex xMAP INTELLIFLEX system. Data was analyzed using the Belysa<sup>®</sup> Immunoassay  
171 Curve Fitting Software (Millipore Sigma). Cytokine production within the BM TME was evaluated  
172 using Isoplexis' CodePlex secretome chips. Briefly, bilateral, tumor-bearing hind limbs (femur  
173 and tibia) were harvested, and BM was collected into 30 µL PBS. Soluble phase fractions were  
174 stored at -80 °C in low-bind Eppendorf tubes until loaded onto a CodePlex secretome chip and  
175 analyzed in an IsoLight instrument.

176

177 *Seahorse:* The day prior to assay CAR T cells were stimulated overnight at an E:T ratio of 2:1.  
178 Cell<sup>®</sup>Tak<sup>®</sup>Coated XF96 microplate was prepared to support testing of cells grown in



179 suspension. Sensor cartridge was hydrated in XF Calibrant and incubated overnight at 37 °C in  
180 a non-CO<sub>2</sub> incubator.

181 On the day of the experiment Seahorse XF DMEM Medium pH 7.4 (Agilent Technologies) was  
182 supplemented with 10 mM glucose, 1 mM pyruvate and 2 mM glutamine for oxygen  
183 consumption rate (OCR) examination and 2mM glutamine for extracellular acidification rate  
184 (ECAR) examination and pre-warmed to 37 °C. Suspension cells were harvested, washed in 1X  
185 PBS, resuspended in the prepared assay media, and gently seeded on the Cell-Tak-Coated  
186 plate at 2 x 10<sup>5</sup> cells/well. The seeded plate was incubated in a 37 °C non-CO<sub>2</sub> incubator for 1  
187 hour prior to the assay. During the incubation, test compounds specific to the assay type were  
188 prepared and added to the ports of the hydrated cartridge. The loaded cartridge was moved to  
189 the XFe96 Analyzer and initial calibration was performed. Following the 1-hour incubation the  
190 Cell-Tak plate was transferred to the Xfe96 Analyzer and the assay was initiated according to  
191 manufacturer's recommendations.

192 All concentrations shown represent final well concentrations:

193 Mito Stress Test (OCR examination)

194 Oligomycin (2.0 µM), FCCP (1.0 µM) and Rotenone/Antimycin A (0.5 µM)

195 Glycolysis Stress Test (ECAR examination)

196 Glucose (10 mM), Oligomycin (1.0 µM) and 2DG (50 mM)

197 T Cell Metabolic Fitness Test

198 First injection of this assay included substrate pathway specific inhibitors:

199 Etomoxir (4.0 µM), long chain fatty acid oxidation

200 UK5099 (2.0 µM), glucose/pyruvate oxidation

201 BPTES (3.0 µM) glutamine oxidation

202 For controls, assay medium was used in port A instead of inhibitors.

203 Following inhibitor injections Oligomycin (1.5 µM), BAM15 (2.5 µM) and Rotenone/Antimycin A  
204 (0.5 µM) were added to all wells.

205 The last injection of each assay included Hoechst 33342 Nuclear Stain to facilitate  
206 Normalization via fluorescent imaging and cell counting supported by the BioTek Cytation 5 Cell  
207 Imaging Multimode Reader. Data was analyzed using the Wave 2.6.1 software and  
208 the Seahorse Analytics cloud-based resource.

209

210 *qRT-PCR*: RNA was isolated using the miRNeasy Mini Kit (Qiagen) and cDNA was synthesized  
211 using SuperScript IV Reverse Transcriptase. Contaminating DNA was removed using Rnase-  
212 Free Dnase (Qiagen) and qPCR was performed using the QuantStudio 6 Flex Real-Time PCR  
213 System with SYBR green (ThermoFisher Scientific). Expression was normalized to TBP, and  
214 relative expression was calculated using the  $\Delta\Delta CT$  formula. Primer sequences are listed in  
215 Supplemental Table 2.

216

217 *NAD<sup>+</sup>/NADH Quantitation*: NADH:NAD<sup>+</sup> ratios were determined using the NAD/NADH-Glo assay  
218 (Promega) according to manufacturer's instructions. Briefly,  $1 \times 10^5$  stimulated CAR T cells were  
219 washed with 1x PBS prior to cell lysis. NAD<sup>+</sup> and NADH levels were quantified independently  
220 using acid/base treatment. Luminescence values were read on a BioTek Synergy H1 plate  
221 reader (Agilent).

222

223 *Mice and in vivo models:*

224 *Systemic Tumor Models*: NOD scid gamma (NSG) mice (NOD.CgPrkdc<sup>scid</sup> Il2rg<sup>tm1Wjl</sup>/SzJ) mice  
225 ages 6-12 weeks were purchased from the Comparative Oncology Shared Resource in-house  
226 mouse colony at Roswell Park. RAG2<sup>-/-</sup> (B6.Cg-Rag2<sup>tm1.1Cgn</sup>/J) mice were purchased from the  
227 Jackson Laboratory and subsequently bred in our facility under the approved protocol 1425M.  
228 NSG mice were intravenously injected with  $1 \times 10^6$  MM.1S-Luc at week -4 and  $3 \times 10^6$  CAR T  
229 cells at week 0. RAG2<sup>-/-</sup> mice were injected with  $2 \times 10^6$  5TGM1<sup>hBCMA</sup>-Luc at week -2 to and  $3 \times$   
230  $10^6$  CAR T cells at week 0 to compensate for differences in tumor engraftment rate amongst the

231 two models. Bioluminescence was measured 2x/week using an IVIS<sup>®</sup> Spectrum In Vivo Imaging  
232 System (PerkinElmer) to assess tumor burden. Mice were injected with 150 mg Luciferin/kg of  
233 body weight and briefly anesthetized through isoflurane inhalation during image acquisition.  
234 Data was analyzed on the Living Image analysis software (PerkinElmer). In some settings,  
235 retroorbital blood collection was performed 1 week after CAR T cell infusion to examine CAR T  
236 cell frequency in circulation. Mice were monitored daily for signs of deteriorating condition or  
237 disease progression including decreased activity, hunched posture, ruffled coat, or hind limb  
238 paralysis and euthanized upon veterinary recommendation.

239 All animal studies were performed in accordance with the Roswell Park Comprehensive Cancer  
240 Center Institutional Animal Care and Use Committee guidelines under the approved protocol  
241 1094M.

242 *CD28<sup>ΔKO</sup>*: *CD28<sup>iKO</sup>* mice were generated by Ozgene (Australia). LoxP sites flanking exon 2 and 3  
243 of the *CD28* gene were introduced to allow for Cre-mediated deletion of the *CD28* gene. Mice  
244 were generously provided by Kelvin Lee (Indiana University) and subsequently bred in-house  
245 under protocol 1425M. Splenocytes were isolated as previously described and CAR T cells were  
246 expanded in the presence of 250 nM 4-hydroxytamoxifen (Sigma-Aldrich) for 4 days to induce  
247 *CD28* deletion.

248 *T-lux*: Transgenic *T-lux* mice generated by Casey Weaver at the University of Alabama at  
249 Birmingham were acquired by Robert McGray (Roswell Park) under a material transfer  
250 agreement (MTA). Mice were utilized as splenocyte donors for CAR T cell manufacturing for *in*  
251 *vivo* imaging of CAR T cell trafficking and expansion.

252  
253 *Statistical analyses*: All statistical analyses were performed using GraphPad Prism software.  
254 Data points represent independent biological replicates. Error bars represent standard deviation  
255 unless otherwise stated. Statistical significance between groups was determined by paired or  
256 unpaired Student's t test, one-way or two-way ANOVA. Survival analysis was performed using a

257 log-rank (Mantel-Cox) test. A p value  $\leq 0.05$  is considered significant: \* $p < 0.05$ , \*\* $p < 0.01$ ,  
258 \*\*\* $p < 0.001$ , \*\*\*\* $p < 0.0001$ .

## 259 Results

### 260 ***Blockade of endogenous CD28 impairs hBCMABB $\zeta$ CAR T cell anti-MM activity.***

261 Since inhibition of the CD28 survival signal in multiple myeloma (MM) cells sensitizes them  
262 to chemotherapy<sup>45,46</sup>, we sought to determine whether CD28 inhibition similarly sensitized MM  
263 cells to killing by CAR T cells. Human CAR T cells targeting BCMA and containing a 4-  
264 1BB/CD3 $\zeta$  intracellular signaling domain (hBCMABB $\zeta$ ) similar to FDA approved CAR products  
265 for MM (Fig. 1A) were generated from healthy donor peripheral blood mononuclear cells  
266 transduced with a previously described retroviral vector<sup>57</sup> (Supplemental Fig. 1A – 1E). Co-  
267 culture of hBCMABB $\zeta$  CAR T cells with human MM cell lines MM.1S or U266, which differ in  
268 their expression profiles of CD28 and B7 ligands (MM.1S = CD28<sup>+</sup>, CD86<sup>+</sup>, CD80<sup>-</sup> & U266 =  
269 CD28<sup>+</sup>, CD86<sup>-</sup>, CD80<sup>-</sup>; Supplemental Fig. 1F), resulted in cytotoxicity across a range of effector  
270 to target ratios (Fig. 1B). Intriguingly, addition of abatacept to co-cultures mildly enhanced  
271 sensitivity of CD86<sup>+</sup> MM.1S, but not CD86<sup>-</sup> U266, to hBCMABB $\zeta$  CAR T cell killing, indicating  
272 that blocking CD28-CD86 interactions on MM cells may sensitize them to CAR T cell therapy  
273 (Fig. 1B). In agreement with potential MM sensitization to CAR T killing, abatacept did not alter  
274 hBCMABB $\zeta$  CAR T cell production of effector cytokines or proinflammatory molecules including  
275 interferon-gamma (IFN- $\gamma$ ), tumor necrosis factor alpha (TNF $\alpha$ ) or granulocyte-macrophage  
276 colony-stimulating factor (GM-CSF) in co-culture assays (Supplemental Fig. 1G).

277 Due to the modest capacity of abatacept to enhance CAR T cell-mediated cytotoxicity *in*  
278 *vitro*, we evaluated the ability of abatacept to enhance hBCMABB $\zeta$  CAR T cell control of  
279 orthotopic CD28<sup>+</sup>, CD86<sup>+</sup> myeloma. Luciferase tagged MM.1S (MM.1S-Luc) cells were  
280 implanted i.v. into NSG hosts followed four weeks later by infusion of  $3 \times 10^6$  hBCMABB $\zeta$  CAR T  
281 cells  $\pm$  3x/weekly injections of abatacept continued until endpoint (Fig. 1C). Bioluminescence  
282 imaging was used to confirm bone marrow engraftment and to normalize average tumor burden

283 across groups immediately prior to therapy. Following hBCMABB $\zeta$  CAR T infusion, MM.1S  
284 burden was assessed by serial bioluminescence imaging. MM regression was observed in all  
285 hBCMABB $\zeta$  CAR T cell treated mice, with most mice apparently tumor free 2 to 3 weeks  
286 following infusion (Fig. 1D). Unexpectedly, MM relapse was more rapidly seen in mice receiving  
287 abatacept + hBCMABB $\zeta$  CAR T cells compared to those receiving single agent hBCMABB $\zeta$   
288 CAR T cells (Fig. 1E), resulting in significantly shorter survival of MM.1S bearing mice in the  
289 abatacept + hBCMABB $\zeta$  CAR T group (Fig. 1F).

290 Prior work has demonstrated that CD28 can contribute to an immunosuppressive MM BME  
291 by interacting with CD80/CD86 on bone marrow resident DCs and inducing production of IL-6  
292 and the tryptophan metabolizing enzyme, indoleamine 2,3-dioxygenase (IDO)<sup>44</sup>. In the low  
293 tumor burden setting, abatacept may function through ligation of B7 family proteins on BMDCs  
294 to create an immunosuppressive MM BME. We therefore repeated CAR T cell  $\pm$  abatacept  
295 treatment regimen in a high MM.1S tumor burden setting in which an immunosuppressive MM  
296 BME should already be established. We found that abatacept similarly accelerated relapse  
297 following hBCMABB $\zeta$  CAR T cell infusion in the high tumor burden setting (Fig. 1G) and  
298 shortened overall survival (Fig. 1H) suggesting that induction of immunosuppression in the MM  
299 bone marrow microenvironment was likely not the primary effect of abatacept exposure.

300

### 301 ***Endogenous CD28 enhances 4-1BB co-stimulated CAR T cell efficacy.***

302 Despite the very clear reduction to *in vivo* CAR T cell efficacy imparted by continuous abatacept  
303 treatment, data shown in Fig. 1 does not differentiate effects of abatacept on cells in the MM  
304 BME versus effects of blocking endogenous CD28 on CAR T cells. To examine CAR T cell  
305 intrinsic effects of endogenous CD28, we generated a tamoxifen inducible CD28 knockout  
306 mouse model (CD28<sup>iKO</sup>) by crossing CD28-floxed mice to mice expressing CreERT2 from the  
307 ROSA26 locus<sup>61</sup>. Following hBCMABB $\zeta$  CAR transduction of CD28<sup>iKO</sup> or littermate control T  
308 cells lacking CreERT2 expression, 4-hydroxytamoxifen was introduced into culture media for 4

309 days to induce CD28 deletion (Fig. 2A). Surface protein expression was evaluated by flow  
310 cytometry over the course of CAR T cell expansion and immediately prior to functional  
311 assessment. Importantly, CD28 surface expression was reduced to near background levels in  
312 CD28<sup>iKO</sup> CAR T cells by 4-OHT exposure (Fig. 2B,2C), while CD4 : CD8 ratio and CAR  
313 expression was unaffected (Supplemental Fig. 2A – 2C). To interrogate functionality of murine  
314 CAR T cells we engineered syngeneic 5TGM1 MM cells to express a chimeric hBCMA-tNGFR  
315 target antigen (5TGM1<sup>hBCMA</sup>)<sup>62-65</sup> (Supplemental Fig. 2D, 2E). Coupling the extracellular  
316 domains of hBCMA to a signaling deficient NGFR transmembrane domain allowed us to  
317 uncouple the target function of BCMA from its survival signal. In co-culture assays, CD28<sup>iKO</sup>  
318 CAR T cells were nearly as effective as control CD28<sup>fl/fl</sup> CAR T cells at killing 5TGM1<sup>hBCMA</sup>  
319 myeloma cells, indicating that endogenous CD28 does not directly impact CAR T cell  
320 cytotoxicity (Fig. 2D). CD28<sup>fl/fl</sup> and CD28<sup>iKO</sup> CAR T cells also produced comparable amounts of  
321 proinflammatory cytokines when stimulated by 5TGM1<sup>hBCMA</sup> *in vitro* (Fig. 2E).

322 In contrast to *in vitro* findings, CD28<sup>iKO</sup> hBCMA<sup>hBCMA</sup>BBmζ CAR T cells differed greatly from  
323 hBCMA<sup>hBCMA</sup>BBmζ CAR T cells generated from littermate controls in their ability to control *in vivo*  
324 myeloma growth. CD28<sup>iKO</sup> hBCMA<sup>hBCMA</sup>BBmζ CAR T cells transiently controlled systemic growth of  
325 luciferase labeled 5TGM1<sup>hBCMA</sup> myeloma in RAG2<sup>-/-</sup> mice while CD28<sup>fl/fl</sup> littermate control  
326 hBCMA<sup>hBCMA</sup>BBmζ CAR T cells demonstrated extended myeloma control (Fig. 2F, 2G). As a result,  
327 the median survival of 5TGM1<sup>hBCMA</sup> myeloma bearing mice treated with CD28<sup>fl/fl</sup> hBCMA<sup>hBCMA</sup>BBmζ  
328 CAR T cells was nearly twice as long as those treated with CD28<sup>iKO</sup> hBCMA<sup>hBCMA</sup>BBmζ CAR T cells  
329 (Fig. 2G, 2H), mirroring effects of abatacept blockade of endogenous CD28 signaling (Fig. 1E,  
330 1F). Moreover, pro-inflammatory cytokines in the MM BME of CD28<sup>iKO</sup> hBCMA<sup>hBCMA</sup>BBmζ CAR T  
331 cell treated mice were substantially reduced (Fig. 2I). These data indicate that CD28<sup>iKO</sup> CAR T  
332 cells did not induce a proinflammatory MM BME despite being able to readily produce pro-  
333 inflammatory cytokines in response to CAR ligation (Fig. 2E).

334

335 ***Endogenous CD28 supports CAR T cell oxidative metabolism.***

336 CD28 controls metabolic reprogramming of activated T cells to enhance production of pro-  
337 inflammatory cytokines and anti-tumor immunity<sup>66-69</sup>. Since CAR T cell efficacy is linked to the  
338 metabolic state of infused cells<sup>70</sup>, we evaluated glycolytic and mitochondrial metabolism of  
339 unstimulated and 5TGM1<sup>hBCMA</sup> stimulated CD28<sup>fl/fl</sup> and CD28<sup>iKO</sup> hBCMAmBBmζ CAR T cells  
340 using Seahorse assays. Changes in extracellular acidification rate (ECAR) in response to  
341 glucose addition or inhibition of mitochondrial ATP synthesis were equivalent between CD28<sup>fl/fl</sup>  
342 and CD28<sup>iKO</sup> CAR T cells (Fig. 3A, 3B), indicating that mBBmζ CAR signaling was sufficient to  
343 induce glycolytic metabolism. In contrast, CD28<sup>iKO</sup> hBCMAmBBmζ CAR T cells displayed  
344 reduced oxygen consumption rate (OCR) and this pattern differed based on stimulation (Fig.  
345 3C,3D). Basal and uncoupled OCR were decreased in unstimulated CD28<sup>iKO</sup> CAR T cells while  
346 uncoupled OCR and spare respiratory capacity (SRC) were decreased in stimulated CD28<sup>iKO</sup>  
347 CAR T cells. Reduced OCR in CD28<sup>iKO</sup> CAR T cells is consistent with the established role of  
348 CD28 in priming mitochondria to support a robust recall response in of memory CD8 T cells<sup>67</sup>.  
349 Yet in contrast to memory CD8 T cells, reduced mitochondrial OCR in CD28<sup>iKO</sup> CAR T cells did  
350 not result from diminished fatty acid oxidation nor from an inability of CD28<sup>iKO</sup> CAR T cells to  
351 oxidize other major anapleurotic substrates glucose and glutamine (Supplemental Fig. 3A).  
352 Moreover, no difference in mitochondria content was observed when comparing CD28<sup>iKO</sup> and  
353 CD28<sup>fl/fl</sup> hBCMAmBBmζ CAR T cells (Supplemental Fig. 3B), further suggesting that  
354 endogenous CD28 signaling regulates mitochondrial oxidative phosphorylation in 4-1BB co-  
355 stimulated CAR T cells.

356 Mitochondrial oxidative phosphorylation relies on the electron carriers NADH to donate  
357 electrons to complex I and FADH<sub>2</sub> to donate electrons to complex II of the electron transport  
358 chain (ETC), driving mitochondrial oxygen consumption and creating a proton gradient across  
359 the inner mitochondria membrane to fuel ATP synthase. Deletion of endogenous CD28 did not  
360 alter the contribution of complex I nor complex II to mitochondrial oxygen consumption by

361 hBCMAMBm $\zeta$  CAR T cells (Supplemental Fig. 3C). Interestingly however, the ratio of NADH to  
362 NAD<sup>+</sup> was increased in target cell stimulated CD28<sup>fl/fl</sup> when compared to CD28<sup>iKO</sup>  
363 hBCMAMBm $\zeta$  CAR T cells (Fig. 3E), indicating that endogenous CD28 signaling increases  
364 ETC substrate availability in 4-1BB co-stimulated CAR T cells. Several crucial metabolic  
365 enzymes reduce NAD<sup>+</sup> to NADH or oxidize NADH to NAD<sup>+</sup> (Fig. 3F), thereby maintaining redox  
366 balance. Quantitative RT-PCR revealed that among these enzymes, only *Gapdh* gene  
367 expression was altered in CD28<sup>iKO</sup> hBCMAMBm $\zeta$  CAR T cells (Fig. 3g). Expression of the  
368 NADP<sup>+</sup> reducing enzymes *ldh1* and *ldh2* were also slightly increased in CD28<sup>iKO</sup>  
369 hBCMAMBm $\zeta$  CAR T cells (Supplemental Fig. 3D). Differences in gene expression, if reflected  
370 in functional enzyme changes, occur in the opposite direction of what would be expected based  
371 on differences in NADH to NAD<sup>+</sup> ratio between CD28<sup>fl/fl</sup> and CD28<sup>iKO</sup> CAR T cells, indicating that  
372 gene expression changes are unlikely to explain the difference in redox state when CD28 is  
373 knocked out of hBCMAMBm $\zeta$  CAR T cells.

374

### 375 ***Endogenous CD28 enhances CAR T cell expansion in the MM BME***

376 Due to the known influence of mitochondrial respiration and redox balance on T cell  
377 proliferation<sup>71,72</sup>, we evaluated proliferation of CD28<sup>fl/fl</sup> and CD28<sup>iKO</sup> CAR T cells. No difference in  
378 proliferation of CD28<sup>fl/fl</sup> and CD28<sup>iKO</sup> CAR T cells was observed over the course of *ex vivo* CAR  
379 manufacture (Fig. 4A). Similarly, expression of the proliferation marker Ki67 induced by co-  
380 culture of CD28<sup>fl/fl</sup> or CD28<sup>iKO</sup> hBCMAMBm $\zeta$  CAR T cells with 5TGM1<sup>hBCMA</sup> target cells was  
381 similar (Fig. 4B). However, when hBCMAMBm $\zeta$  CAR T cells in the MM BME or peripheral  
382 blood were enumerated 7 days after adoptive transfer into 5TGM1<sup>hBCMA</sup> bearing mice (Fig. 4C),  
383 a large decrease in CD4<sup>+</sup> CD28<sup>iKO</sup> CAR T cells was observed (Fig. 4D, 4E, Supplemental Fig.  
384 4A). Importantly, CD28<sup>iKO</sup> hBCMAMBm $\zeta$  CAR T cells maintained low/negative CD28 surface  
385 expression in the MM BME (Fig. 4F). Abatacept similarly reduced the frequency of human CD4<sup>+</sup>  
386 hBCMABB $\zeta$  CAR T cells in the MM BME of MM.1S bearing mice (Fig. 4G), while it had no effect



387 on human CAR T cells in the peripheral blood (Fig. 4H). The frequency of CD8<sup>+</sup> CAR T cells in  
388 the MM BME or peripheral blood was unaffected by CD28 knockout or abatacept treatment (Fig.  
389 4D – 4H).

390 The observed reduction in CD4<sup>+</sup> CAR T cells in the MM BME upon deletion or blockade of  
391 endogenous CD28 led us to test whether endogenous CD28 signaling contributes to *in vivo*  
392 expansion of luciferase expressing hBCMABBζ CAR T cells generated from T-lux mice<sup>73</sup>.  
393 Approximately one week after infusion, which aligns with the kinetics of tumor regression, T-lux  
394 hBCMABBmζ CAR T cell luminescence within the hind limbs of 5TGM1<sup>hBCMA</sup> myeloma bearing  
395 mice rapidly increased with a signal plateau observed approximately 1 week later (Fig. 4I, 4J).  
396 Abatacept treatment significantly blunted *in vivo* expansion of T-lux hBCMABBmζ CAR T cells  
397 in the MM BME (Fig. 4I), suggesting that CD28 signaling supports *in vivo* expansion of 4-1BB  
398 co-stimulated CAR T cells.

399

#### 400 ***Transient CD28 blockade reduces inflammatory cytokines in the MM BME***

401 Since endogenous CD28 promoted *in vivo* hBCMABBmζ CAR T cell expansion and  
402 inflammatory cytokine production in the MM BME, we sought to test whether abatacept  
403 blockade of CD28 ligation could lessen the severity of CAR T associated cytokine release. To  
404 this end, myeloma bearing mice were treated with abatacept for 1 week following CAR T cell  
405 infusion (Fig. 5A). At this early timepoint, abatacept had no effect on anti-tumor activity of BCMA  
406 targeted human or mouse CAR T cells (Fig. 5B, Supplemental Fig. 4B) and only a very minor  
407 effect on MM BME levels of human inflammatory cytokines in the MM BME (Fig. 5C). Since  
408 human cytokines could only come from CAR T cells or MM.1S cells, and most cytokines  
409 measured are not known to be made by MM cells, we concluded that CD28 blockade with  
410 abatacept did not affect *in vivo* CAR T cell cytokine secretion nor anti-tumor activity in the first  
411 week following infusion.

412 Somewhat surprisingly, inflammatory cytokine levels in the MM BME were dramatically  
413 reduced by CD28 deletion from mouse hBCMAmBBm $\zeta$  CAR T cells (Fig. 2I) yet unaffected by  
414 CD28 blockade using abatacept in human hBCMABB $\zeta$  CAR T cell treated mice (Fig. 5C). Such  
415 divergent findings may be due to contributions of cells other than CAR T cells to the mouse MM  
416 BME cytokine milieu or differences between how blockade of CD28 with abatacept and deletion  
417 of CD28 affect 4-1BB co-stimulated CAR T cells. To address these possibilities, we measured  
418 murine inflammatory cytokine levels in the MM BME of mouse hBCMAmBBm $\zeta$  CAR T cell  
419 treated 5TGM1<sup>hBCMA</sup> bearing mice. Abatacept diminished levels of murine inflammatory  
420 cytokines in the MM BME of hBCMAmBBm $\zeta$  CAR T cell treated mice (Fig. 5D), yet not to the  
421 extent of CD28 deletion.

422 Notable among inflammatory cytokines affected by both abatacept treatment and CD28  
423 deletion were IP-10, which is secreted by monocytes and stromal cells in response to IFN- $\gamma$ <sup>74</sup>,  
424 and IL-12, which is mainly secreted by monocytes, macrophages, neutrophils, and dendritic  
425 cells<sup>75</sup>. It is therefore likely that other cells contribute to murine inflammatory cytokine production  
426 in the MM BME of hBCMAmBBm $\zeta$  CAR T cell treated mice and given the magnitude of cytokine  
427 changes, that there is also a difference between how abatacept treatment and deletion of CD28  
428 affects cytokine production.

429

#### 430 ***Transient CD28 blockade does not inhibit hBCMABB $\zeta$ anti-MM activity.***

431 Based on our observation that abatacept could limit pro-inflammatory cytokine release but  
432 not early anti-tumor activity of hBCMABB $\zeta$  CAR T cells, we predicted that transient abatacept  
433 exposure would not impair survival of myeloma bearing mice. To test this, abatacept was  
434 administered to MM.1S tumor bearing NSG mice from day -1 to day 7 post hBCMABB $\zeta$  CAR T  
435 cell infusion (Fig. 5F). Transient abatacept exposure resulted in a slight reduction in tumor  
436 regression induced by hBCMABB $\zeta$  CAR T cells (Supplemental Fig. 4C) but did not affect the  
437 long-term survival of hBCMABB $\zeta$  CAR T cell treated myeloma bearing mice (Fig. 5H).

438

## 439 Discussion

440 CAR T cell therapies targeting BCMA have shown curative potential in patients with  
441 relapsed/refractory multiple myeloma (MM)<sup>25,27</sup>. However, achieving long-term remissions  
442 remains an ongoing challenge, with one-quarter to greater than one-half of patients  
443 experiencing myeloma relapse within one year of CAR T infusion. In this study we set out to  
444 determine whether CD28 blockade using abatacept could sensitize MM cells to CAR T cell  
445 therapy in a manner analogous to standard chemotherapy<sup>45,46,50</sup>. In contrast to expectations, we  
446 found that abatacept limited efficacy of clinically relevant BCMA targeted, 4-1BB co-stimulated  
447 CAR T cells in an established human xenograft myeloma mouse model. Using a novel CD28  
448 inducible knockout mouse model to generate CD28-deficient (CD28<sup>iKO</sup>) CAR T cells, we further  
449 revealed a previously unrecognized role for the endogenous CD28 receptor on 4-1BB co-  
450 stimulated CAR T cells. CD28 deletion did not alter BCMA targeted, 4-1BB co-stimulated CAR T  
451 cell cytotoxic capabilities nor alter inflammatory cytokine production *in vitro*, but rather resulted  
452 in diminished mitochondrial metabolism and a lower ratio of the oxidized form of nicotinamide  
453 adenine dinucleotide (NADH) to its reduced form (NAD<sup>+</sup>). These metabolic changes were  
454 associated with limited *in vivo* expansion of CD28<sup>iKO</sup> 4-1BB co-stimulated CAR T cells and a  
455 reduction in CAR T cell induced inflammatory cytokine production in the multiple myeloma bone  
456 marrow microenvironment (MM BME). Abatacept treatment similarly reduced *in vivo* 4-1BB co-  
457 stimulated CAR T cell expansion and inflammatory cytokine production. Importantly however,  
458 short-term blockade of endogenous CD28 using abatacept during the first week following CAR T  
459 cell infusion reduced inflammatory cytokine levels in the MM BME without altering long-term  
460 survival of BCMA targeted, 4-1BB co-stimulated CAR T cell treated myeloma bearing mice.

461 Robust CAR T cell activation and expansion can induce systemic toxicities, including  
462 cytokine release syndrome (CRS), immune effector cell-associated neurotoxicity syndrome  
463 (ICANS), and immune effector cell-associated hematologic toxicity (ICAHT)<sup>76-78</sup>. In pivotal CAR

464 T trials in MM<sup>25,27</sup>, 76 – 84% of patients experienced CRS, 18 – 21% experienced ICANS, and  
465 nearly all patients experienced hematologic toxicity, although these were generally transient.  
466 Current treatment options for CRS and ICANS include IL-6 receptor blockade with tocilizumab,  
467 corticosteroids for tocilizumab refractory cases, and the anti-IL-6 antibody siltuximab for  
468 tocilizumab and corticosteroid refractory toxicities<sup>79</sup>. Additionally, the IL-1 receptor antagonist  
469 anakinra is being explored as a potential prophylactic treatment to prevent CRS and ICANS<sup>80</sup>.  
470 Data presented here raise the possibility that abatacept (CTLA4-Ig), which is FDA approved for  
471 the treatment of rheumatoid arthritis, juvenile idiopathic arthritis, and psoriatic arthritis along with  
472 prevention of acute graft versus host disease<sup>81,82</sup>, may also be useful as prophylactic treatment  
473 to prevent toxicities brought on by 4-1BB co-stimulated CAR T cells. Whether abatacept could  
474 have similar utility in preventing CD28 co-stimulated CAR T cell toxicities is an open question  
475 currently lacking clinical relevance in the setting of multiple myeloma, where both FDA approved  
476 CAR designs contain a 4-1BB co-stimulatory domain.

477 Co-stimulation has long been known to be critical for anti-tumor effects of CAR T cells<sup>83,84</sup>,  
478 with different CAR-encoded co-stimulatory domains having distinct effects on CAR T cell  
479 properties<sup>17</sup>. Clinically available CARs contain either a CD28 or a 4-1BB co-stimulatory domain.  
480 CD28 co-stimulated CAR T cells exhibit rapid anti-tumor effector function but lack functional  
481 persistence associated with 4-1BB co-stimulated CAR T cells. Modulation of CAR-encoded  
482 CD28 signaling has resulted in improved functional persistence and reduced CAR T cell  
483 exhaustion in pre-clinical models<sup>85,86</sup>. Recent studies have hinted at a role for endogenous  
484 CD28 in determining CAR T cell efficacy. However, evidence for endogenous CD28 modulation  
485 of CAR T cell function was either indirect, in the case of CTLA4 knockout<sup>55</sup>, or complicated by  
486 co-expression of IL-12 from a fourth-generation armored CAR construct<sup>87</sup>. Data presented here  
487 provide the first direct evidence that endogenous CD28 affects efficacy of second-generation, 4-  
488 1BB co-stimulated CAR T cells comparable to those used to treat myeloma patients. These data

489 raise important questions about how signaling from CAR co-stimulatory domains interfaces with  
490 signaling from endogenous co-stimulatory, and/or co-inhibitory receptors.

491 In light of recent evidence that CD28 co-stimulation in the tumor microenvironment is critical  
492 for effector differentiation and anti-tumor function of cytotoxic T cells<sup>56,88</sup>, the context in which  
493 endogenous CD28 expressed on 4-1BB co-stimulated CAR T cells encounters ligands may  
494 influence anti-tumor efficacy and/or inflammatory cytokine production. B lineage tumors targeted  
495 clinically by CAR T cells are characterized by high levels of CD28 ligand expression, with CD80,  
496 CD86, or both expressed on tumor cells in more than half of myeloma, non-Hodgkin's  
497 lymphoma, and B-ALL patients<sup>89-91</sup>. CD80 and CD86 are also expressed on antigen presenting  
498 cells throughout the body of cancer patients and may have similar or disparate effects on CAR T  
499 cells, likely based on whether CAR engagement occurs concurrently with CD28 engagement. If  
500 future studies find that the context in which endogenous CD28 is engaged matters, CD80 and/or  
501 CD86 expression patterns may become useful in determining whether CD28 or 4-1BB co-  
502 stimulated CAR T cells are used to treat particular patients.

503 Overall, results presented here provide the first direct evidence that endogenous CD28 is  
504 important for driving anti-tumor function of 4-1BB co-stimulated CAR T cells. These results raise  
505 many interesting and important biological questions about co-stimulation and signaling in CAR T  
506 cells and, perhaps more importantly raise the possibility that blocking endogenous CD28  
507 signaling may abrogate some of the toxic side effects associated with CAR T therapy. Future  
508 studies aimed at optimizing methods and timing of CD28 blockade have the potential to lead to  
509 improved clinical strategies for limit toxicities while maintaining CAR T cell efficacy.

510

## 511 **Acknowledgements**

512 The authors would like to thank Steven Turowski and Joseph Sperryak of the Translational  
513 Imaging Shared Resource (TISR) at Roswell Park for their assistance with bioluminescent  
514 imaging studies as well as the Cancer Center Support Grant: P30CA016056 and shared

515 instrumentation grant: S10OD16450. We would also like to acknowledge Courtney Ryan for her  
516 technical expertise and operation of the Seahorse XFe96 extracellular flux analyzer within the  
517 Immune Analysis Facility at Roswell Park. Finally, we would like to thank Bristol Myers Squibb  
518 (BMS) for providing abatacept for use in our studies under the non-sponsored research  
519 agreement IM101-902.

520

## 521 **Author Contributions**

522 **Conception and design:** M. Lieberman, K. Lee, S. Olejniczak

523 **Development of methodology:** M. Lieberman, K. Lee, S. Olejniczak

524 **Acquisition of data (provided animals, managed studies, provided facilities, etc.):** M.  
525 Lieberman, J. Bramson, R. Brentjens, K. Lee, S. Olejniczak

526 **Analysis and interpretation of data:** M. Lieberman, K. Lee, S. Olejniczak

527 **Writing, review, and/or revision of the manuscript:** M. Lieberman, K. Lee, S. Olejniczak

528 **Administrative, technical, or material support:** M. Lieberman, J. Tong, N. Odukwe, T.  
529 Purdon, R. Burchett, A.J.R. McGray, B. Gillard, C. Brackett, C. Chavel

530 **Study supervision:** S. Olejniczak

531 All authors have read and agreed to the published version of the manuscript.

532

## 533 **Funding**

534 Services and resources were provided by the Flow and Image Cytometry Shared Resource, the  
535 Translational Imaging Shared Resource (TISR), and the Experimental Tumor Model Shared  
536 Resource at Roswell Park. All Roswell Park shared resources were supported through NIH  
537 National Cancer Institute Cancer Center Support Grant P30CA016056. This work was  
538 supported by the U.S. National Institutes of Health (NIH) grants R03CA256122 and  
539 R01AI155499 awarded to S.H.O., and the NIH Institutional National Research Service Award  
540 Training Grant T32CA085183 awarded to M.M.L.

541

542 **Institutional Review Board Statement**

543 This study involves de-identified healthy donor samples collected under an approved protocol  
544 reviewed by the Roswell Park Institutional Review Board (IRB): BDR 115919. All animal  
545 experiments were performed in accordance with the Institutional Animal Care and Use  
546 Committee (IACUC) guidelines and were approved under experimental IACUC protocol: 1094M.

547

548 **Data Availability Statement**

549 All data associated with this paper are included in the manuscript and supplementary  
550 materials. Requests for resources and reagents should be directed to and will be fulfilled by the  
551 corresponding author, Scott H. Olejniczak ([scott.olejniczak@roswellpark.org](mailto:scott.olejniczak@roswellpark.org))

552

553 **Conflicts of Interest**

554 R.J.B. has licensed intellectual property to and collects royalties from Bristol Myers Squibb  
555 (BMS), Caribou, and Sanofi. R.J.B. received research funding from BMS. R.J.B. is a consultant  
556 to BMS, Atara Biotherapeutics Inc, and Triumvira. R.J.B is a member of the scientific advisory  
557 board for Triumvira.

558 **Figure Legends:**

559 **Figure 1: Endogenous CD28 blockade impairs hBCMABBζ CAR T cell anti-myeloma**  
560 **efficacy.**

561 **(A)** Schematic of second-generation retroviral CAR construct used to generate BCMA targeted  
562 human CAR T cells.

563 **(B)** CAR T cell cytotoxic activity during a 24-hr. co-culture with luciferase-tagged MM.1S (left) or  
564 U266 (right) myeloma cells ± abatacept. Data are shown as mean ± SD and representative  
565 of hBCMABBζ CAR T cells generated from 3 healthy donors. \* $p < 0.05$  by two-way analysis  
566 of variance (ANOVA) with Tukey's multiple comparison test.

567 **(C)** Diagram of experimental setup used to evaluate hBCMABBζ CAR T + abatacept therapy in  
568 a human MM xenograft model. NSG mice were intravenously inoculated with  $1 \times 10^6$   
569 MM.1S-luc myeloma cells on day -28 and treated with CAR T cells on day 0. Mice received  
570 200 µg abatacept 3x/week beginning the day before infusion and continuing through  
571 endpoint. Tumor burden was monitored by IVIS bioluminescent imaging (BLI) 2x/week.

572 **(D)** Representative bioluminescent images of MM.1S bearing mice on specified days following  
573 CAR T cell infusion.

574 **(E)** Tumor burden expressed as relative photon flux measured by BLI from MM.1S-luc bearing  
575 mice treated with hBCMABBζ CAR T or control T cells ± abatacept (200 µg, 3x/week). Each  
576 line represents an individual mouse ( $n = 7$  mice per CAR T cell treated group).

577 **(F)** Kaplan – Meier analysis of survival of hBCMABBζ CAR T or control T cells ± abatacept (200  
578 µg, 3x/week) treated MM.1S-luc bearing mice ( $n = 8 - 12$  mice per CAR T cell treated  
579 group). Median survival of hBCMABBζ CAR T treated mice was >100 days post CAR T cell  
580 infusion vs. 55 days for hBCMABBζ CAR T + abatacept treated mice. \*\*\*\* $p < 0.0001$  by log-  
581 rank Mantel-Cox test.

582 **(G)** Tumor burden expressed as relative photon flux measured by BLI from MM.1S high tumor  
583 burden mice (inoculated on day -35) treated with hBCMABBζ CAR T or control T cells ±



584 abatacept (200 µg, 3x/week). Each line represents an individual mouse (n = 4 mice per  
585 CAR T cell treated group).

586 **(H)** Kaplan – Meier analysis of survival of hBCMABBζ CAR T or control T cells ± abatacept (200  
587 µg, 3x/week) treated MM.1S-luc high tumor burden mice (n = 4 mice per group). Median  
588 survival of hBCMABBζ CAR T treated mice was 80 days vs. 45 days for hBCMABBζ CAR  
589 T + abatacept treated mice. \*\*\*p<0.0001 by log-rank Mantel-Cox test.

590

591 **Figure 2: CD28<sup>iKO</sup> hBCMABBmζ CAR T cells are functionally impaired *in vivo*.**

592 **(A)** Schematic depicting the process of manufacturing mouse CD28 knockout (CD28<sup>iKO</sup>)  
593 hBCMABBmζ CAR T cell.

594 **(B)** Surface CD28 protein expression on CD28<sup>fl/fl</sup> versus CD28<sup>iKO</sup> mouse T cells during CAR T  
595 cell manufacture.

596 **(C)** Median fluorescent intensity (MFI) of CD28 measured by flow cytometry at the conclusion of  
597 CD28<sup>fl/fl</sup> versus CD28<sup>iKO</sup> mouse CAR T manufacture. Data shown as mean ± SD from 10+  
598 independent experiments. \*p<0.05, \*\*\*\*p<0.0001 by one-way ANOVA.

599 **(D)** CD28<sup>fl/fl</sup> versus CD28<sup>iKO</sup> hBCMABBmζ CAR T cell cytotoxic activity during 24 hr. co-culture  
600 with luciferase-tagged 5TGM1<sup>hBCMA</sup> mouse myeloma cells. Cell viability was assessed by  
601 luciferase assay. Data are shown as mean ± SD and representative of at least 3  
602 independent experiments. \*p<0.05, \*\*p<0.01 by two-way ANOVA with Tukey's multiple  
603 comparison test.

604 **(E)** Heatmap representation of culture supernatant mouse cytokine concentrations measured by  
605 multiplexed Luminex assays at the conclusion of a 24-hr. co-culture of hBCMABBmζ  
606 CD28<sup>fl/fl</sup> or CD28<sup>iKO</sup> CAR T cells with 5TGM1<sup>hBCMA</sup> myeloma cells. Log<sub>2</sub> transformed cytokine  
607 concentrations represent the mean of 4 independent experiments.

608 **(F)** Diagram of experimental setup used to evaluate CD28<sup>fl/fl</sup> versus CD28<sup>iKO</sup> hBCMABBmζ  
609 CAR T cell therapy in a mouse MM xenograft model. RAG2<sup>-/-</sup> mice were inoculated

610 intravenously with  $2 \times 10^6$  5TGM1<sup>hBCMA</sup>-luc cells on day -14 and treated with CD28<sup>fl/fl</sup> or  
611 CD28<sup>iKO</sup> CAR T cells on day 0. Tumor burden was monitored by IVIS bioluminescent  
612 imaging (BLI) 2x/week through endpoint.

613 **(G)** Tumor burden expressed as relative photon flux measured by BLI from 5TGM1<sup>hBCMA</sup>-luc  
614 bearing mice treated with CD28<sup>fl/fl</sup> or CD28<sup>iKO</sup> hBCMAmBBm $\zeta$  CAR T or control T cells. Each  
615 line represents an individual mouse (n = 6 mice per CAR T cell treated group).

616 **(H)** Kaplan – Meier analysis of survival of CD28<sup>fl/fl</sup> or CD28<sup>iKO</sup> hBCMAmBBm $\zeta$  CAR T cell or  
617 control T cell treated 5TGM1<sup>hBCMA</sup>-luc bearing mice (n = 6 mice per CAR T cell treated  
618 group). Median survival of CD28<sup>fl/fl</sup> hBCMAmBBm $\zeta$  CAR T treated mice was 38 days post-  
619 CAR T cell infusion vs. 24 days for CD28<sup>iKO</sup> hBCMAmBBm $\zeta$  CAR T treated mice. \*p<0.05,  
620 \*\*p<0.01, \*\*\*p<0.001 by log-rank Mantel-Cox test.

621 **(I)** Heatmap representation of cytokine levels in the MM BME 7 days following infusion of  
622 CD28<sup>fl/fl</sup> or CD28<sup>iKO</sup> hBCMAmBBm $\zeta$  CAR T cells into 5TGM1<sup>hBCMA</sup>-luc bearing mice. Bilateral  
623 hind limbs were harvested, and BM was flushed into 15  $\mu$ L PBS for multiplexed cytokine  
624 analysis. Log<sub>2</sub> transformed cytokine concentrations represent the mean of 3 mice per group.

625

626 **Figure 3: Perturbation of oxidative metabolism and redox homeostasis in stimulated**  
627 **CD28<sup>iKO</sup> hBCMAmBBm $\zeta$  CAR T cells.**

628 **(A)** Representative Seahorse Glycolysis Stress Test performed 24 hr. after stimulation of  
629 CD28<sup>fl/fl</sup> or CD28<sup>iKO</sup> hBCMAmBBm $\zeta$  CAR T cells with 5TGM1<sup>hBCMA</sup> myeloma cells.  
630 Connected data points represent mean extracellular acidification rate (ECAR)  $\pm$  SD of four  
631 technical replicates at indicated time points during a representative experiment that was  
632 repeated at least 3 times. Dashes indicate the timing of glucose, oligomycin (Oligo) and 2-  
633 deoxyglucose (2-DG) injection.

634 **(B)** Quantified rates of glycolysis (left), glycolytic capacity (middle), and glycolytic reserve (left)  
635 in CD28<sup>fl/fl</sup> or CD28<sup>iKO</sup> hBCMAmBBm $\zeta$  CAR T cells  $\pm$  24-hr. stimulation with 5TGM1<sup>hBCMA</sup>

636 myeloma cells. Bars represent mean  $\pm$  SD, dots represent independent experiments. ns =  
637 not significant by one-way ANOVA.

638 **(C)** Representative Seahorse Mito Stress Test performed 24 hr. after stimulation of CD28<sup>fl/fl</sup> or  
639 CD28<sup>iKO</sup> hBCMAmBBm $\zeta$  CAR T cells with 5TGM1<sup>hBCMA</sup> myeloma cells. Connected data  
640 points represent mean oxygen consumption rate (OCR)  $\pm$  SD of four technical replicates at  
641 indicated time points during a representative experiment that was repeated at least 3 times.  
642 Dashes indicate the timing of oligomycin (Oligo), FCCP, and rotenone (Rot) + antimycin A  
643 (Ant. A) injection.

644 **(D)** Quantified basal OCR (right), uncoupled maximal respiration (middle), and spare respiratory  
645 capacity (SRC) expressed as percent of basal OCR (left) in CD28<sup>fl/fl</sup> or CD28<sup>iKO</sup>  
646 hBCMAmBBm $\zeta$  CAR T cells  $\pm$  24 hr. stimulation with 5TGM1<sup>hBCMA</sup> myeloma cells. Bars  
647 represent mean  $\pm$  SD, dots represent independent experiments. \* $p$ <0.05, \*\* $p$ <0.01 by one-  
648 way ANOVA.

649 **(E)** Ratio of NADH to NAD<sup>+</sup> ratios in CD28<sup>fl/fl</sup> or CD28<sup>iKO</sup> hBCMAmBBm $\zeta$  CAR T cells prior to 4-  
650 OHT mediated CD28 deletion or  $\pm$  24 hr. stimulation with 5TGM1<sup>hBCMA</sup> myeloma cells. Bars  
651 represent mean  $\pm$  SD from 3 independent experiments. \* $p$ <0.05 by paired Student's  $t$  test.

652 **(F)** Diagrams depicting enzymes of central carbon metabolism that interconvert NADH and  
653 NAD<sup>+</sup>.

654 **(G)** Relative expression of mRNAs coding enzymes depicted in (F) in CD28<sup>iKO</sup> versus CD28<sup>fl/fl</sup>  
655 hBCMAmBBm $\zeta$  CAR T cells following 24 hr. stimulation with 5TGM1<sup>hBCMA</sup> myeloma cells.  
656 Bars represent mean log<sub>2</sub> transformed  $\Delta\Delta$ Ct values  $\pm$  SD, dots technical replicates pooled  
657 from 3 independent experiments. *Tbp* and *Actb* were used as endogenous controls.  
658 \*\*\*\* $p$ <0.0001 by two-way ANOVA.

659

660 **Figure 4: Diminished *in vivo* expansion of 4-BB co-stimulated CD28<sup>iKO</sup> CAR T cells.**

- 661 **(A)** Expansion of CD28<sup>fl/fl</sup> versus CD28<sup>iKO</sup> hBCMAmBBmζ CAR T cells over the course of  
662 manufacturing. ns = not significant by two-way ANOVA.
- 663 **(B)** Expression of the proliferation marker Ki-67 in CD28<sup>fl/fl</sup> versus CD28<sup>iKO</sup> hBCMAmBBmζ CAR  
664 T cells following 24 hr. stimulation with 5TGM1 target cells as assessed by flow cytometric  
665 analysis. ns = not significant by one-way ANOVA.
- 666 **(C)** Diagram of experimental setup. 5TGM1<sup>hBCMA</sup> bearing RAG2<sup>-/-</sup> mice were treated with CD28<sup>fl/fl</sup>  
667 or CD28<sup>iKO</sup> hBCMAmBBmζ CAR T cells (4D and 4E) or MM.1S bearing NSG mice were  
668 treated with hBCMABBζ CAR T cells ± 200µg abatacept on days -1, 1, 3, 5, 7 (4F) and  
669 euthanized 7 days post adoptive transfer for blood collection and hind limb BM harvest.
- 670 **(D)** CAR T cell frequency assessed by flow cytometry in bone marrow (BM, left) and peripheral  
671 blood (right) one week after adoptive transfer of CD28<sup>fl/fl</sup> or CD28<sup>iKO</sup> hBCMAmBBmζ CAR T  
672 cells into 5TGM1<sup>hBCMA</sup> myeloma bearing mice. Bars represent mean ± SD, dots indicate  
673 individual mice (n = 3-6 mice per group). \*\*p<0.01, \*\*\*\*p<0.0001 by two-way ANOVA with  
674 Tukey's multiple comparison test.
- 675 **(E)** CD28 surface protein expression on BM-infiltrating CD28<sup>fl/fl</sup> or CD28<sup>iKO</sup> hBCMAmBBmζ CAR  
676 T cells one week after adoptive transfer into 5TGM1<sup>hBCMA</sup> myeloma bearing mice.
- 677 **(F)** CAR T cell frequency assessed by flow cytometry in bone marrow (BM, left) and peripheral  
678 blood (right) one week after adoptive transfer of hBCMABBζ CAR T cells into MM.1S  
679 myeloma bearing mice ± abatacept. CAR T population identified by surface staining and  
680 analyzed by flow cytometry. Bars represent mean ± SD, dots indicate individual mice (n = 4-  
681 5 mice per group). \*\*\*p<0.001 by two-way ANOVA with Tukey's multiple comparison test.
- 682 **(G)** Representative IVIS bioluminescence images of T-lux luciferase expressing hBCMAmBBmζ  
683 CAR T cells ± abatacept (200µg, 3x/week) on day 7 or day 15 after infusion.
- 684 **(H)** Quantification of photon flux by IVIS imaging within the hind limb region of interest (ROI)  
685 over a four-week period following T-lux hBCMAmBBmζ CAR T cell infusion ± abatacept  
686 (200µg, 3x/week) into 5TGM1<sup>hBCMA</sup> myeloma bearing mice. Dots represent individual mice (n

687 = 3 mice per group), lines are best-fit sigmoidal curves, and significance was determined by  
688 mixed effects modeling.

689

690 **Figure 5: Transient CD28 blockade limits inflammatory cytokines in the MM BME without**  
691 **affecting survival of hBCMAmBBm $\zeta$  CAR T cell treated mice.**

692 **(A)** Diagram of experimental setup. MM.1S bearing NSG mice were treated with hBCMAmBB $\zeta$   
693 CAR T cells  $\pm$  200 $\mu$ g abatacept on days -1, 1, 3, 5, 7 (5B and 5C) or 5TGM1<sup>hBCMA</sup> bearing  
694 RAG2<sup>-/-</sup> mice were treated with CD28<sup>fl/fl</sup> or CD28<sup>iKO</sup> hBCMAmBBm $\zeta$  CAR T cells (5D and 5E)  
695 and euthanized 7 days post adoptive transfer for hind limb BM harvest.

696 **(B)** Myeloma burden assessed by flow cytometry for human CD138<sup>+</sup> cells in the bone marrow of  
697 MM.1S bearing mice treated as described in 5A. Bars represent mean  $\pm$  SD, dots indicate  
698 individual mice. \*\*p<0.01 by one-way ANOVA, ns = not significant.

699 **(C)** Heatmap representation of human cytokine levels in the MM BME 7 days after treatment of  
700 MM.1S bearing mice with hBCMAmBB $\zeta$  CAR T cells  $\pm$  abatacept. Bilateral hind limbs were  
701 harvested, and BM was flushed into 15  $\mu$ L PBS for multiplexed cytokine analysis. Log<sub>2</sub>  
702 transformed cytokine concentrations represent the mean of 3-6 mice per group.

703 **(D)** Heatmap representation of murine cytokine levels in the MM BME 7 days after treatment of  
704 5TGM1<sup>hBCMA</sup> bearing mice with hBCMAmBBm $\zeta$  CAR T cells  $\pm$  abatacept. Bilateral hind limbs  
705 were harvested, and BM was flushed into 15  $\mu$ L PBS for multiplexed cytokine analysis. Log<sub>2</sub>  
706 transformed cytokine concentrations represent the mean of 2-3 mice per group.

707 **(E)** Bar graphs showing concentrations of murine IP-10 (left) and IL-12 (right) in the MM BME 7  
708 days after treatment of 5TGM1<sup>hBCMA</sup> bearing mice with CD28<sup>fl/fl</sup> hBCMAmBBm $\zeta$  CAR T cells  
709  $\pm$  abatacept versus CD28<sup>iKO</sup> hBCMAmBBm $\zeta$  CAR T cells. Bars represent mean  $\pm$  SD of 2-3  
710 biological replicates. \*\*p<0.01, \*\*\*p<0.001 by one-way ANOVA.

711 **(F)** Diagram of experimental setup. MM.1S bearing NSG mice were treated with hBCMABBζ  
712 CAR T cells ± 200µg abatacept on days -1, 1, 3, 5, 7 and tumor burden was monitored by  
713 bioluminescent imaging 2x/week until endpoint.

714 **(G)** Kaplan – Meier analysis of survival of hBCMABBζ CAR T ± transient abatacept or mock  
715 transduced T cell treated MM.1S-luc bearing mice (n = 4-5 mice per CAR T cell treated  
716 group). Median survival of hBCMABBζ CAR T treated mice was >100 days post CAR T cell  
717 infusion vs. 97 days for hBCMABBζ CAR T + transient abatacept treated mice. Statistical  
718 significance was determined by log-rank Mantel-Cox test.

719 **Supplemental Figure Legends:**

720 **Supplemental Fig. 1: Characterization of human hBCMABB $\zeta$  CAR T cells and myeloma**  
721 **target cells.**

722 **(A)** CD4:CD8 ratio in CAR T cell infusion products generated from PBMCs of healthy donors.

723 Relative frequency of CD4<sup>+</sup> and CD8<sup>+</sup> CAR T cells assessed by flow cytometry. Each data  
724 point represents an independent donor (n = 8).

725 **(B)** Representative flow cytometry dot plot depicting the frequency of CAR transduced cells.

726 **(C)** Transduction efficiency (left) and mean fluorescence intensity MFI; right) of hBCMABB $\zeta$   
727 CAR expression on human CD3<sup>+</sup> T cells determined using  $\alpha$ G4S linker antibody and flow  
728 cytometry. Dots represent independent donors (n = 10).

729 **(D)** Surface CD28 protein expression on CD4<sup>+</sup> and CD8<sup>+</sup> hBCMABB $\zeta$  CAR T cells determined  
730 by MFI. Each data point represents an independent donor (n = 6). \*\*p<0.01 by unpaired  
731 Student's t test \*\*p<0.01.

732 **(E)** Flow cytometry histograms depicting surface expression of MM defining phenotypic  
733 markers CD138 and BCMA along with co-receptors CD28, CD80, and CD86 on human MM  
734 cell lines, MM.1S and U266.

735 **(F)** Heatmap representation of culture supernatant human cytokine concentrations measured  
736 by multiplexed Luminex assays at the conclusion of a 24-hr. co-culture of hBCMABB $\zeta$  CAR  
737 T cells  $\pm$  abatacept with MM.1S myeloma cells. Log<sub>2</sub> transformed cytokine concentrations  
738 represent the mean of 5 independent experiments using CAR T cells generated from 5  
739 healthy donors.

740

741 **Supplemental Fig. 2: Characterization of mouse CD28<sup>iKO</sup> hBCMAMBm $\zeta$  CAR T cells and**  
742 **myeloma target cells.**

- 743 **(A)** CD4:CD8 ratio in CAR T cell infusion products generated from CD28<sup>fl/fl</sup> or CD28<sup>iKO</sup>  
744 splenocytes. Relative frequency of CD4<sup>+</sup> and CD8<sup>+</sup> CAR T cells assessed by flow  
745 cytometry. Each data point represents an independent experiment (n = 6 per group).
- 746 **(B)** Representative flow cytometry histograms depicting CD28<sup>fl/fl</sup> and CD28<sup>iKO</sup> hBCMAmBBmζ  
747 CAR transduced T cells.
- 748 **(C)** Transduction efficiency of the hBCMAmBBmζ CAR into CD28<sup>fl/fl</sup> versus CD28<sup>iKO</sup> mouse T  
749 cells, expressed as percentage of CD3<sup>+</sup> T cells determined using αG4S linker antibody and  
750 flow cytometry. Dots represent independent experiments (n ≥ 10 per group).
- 751 **(D)** Schematic of lentiviral vector used to transduce 5TGM1 cells to express human BCMA  
752 (hBCMA) and firefly luciferase.
- 753 **(E)** Flow cytometry histogram depicting surface hBCMA expression on transduced and sorted  
754 5TGM1 mouse myeloma cells.

755

756 **Supplemental Fig. 3:**

- 757 **(A)** CD28<sup>fl/fl</sup> and CD28<sup>iKO</sup> mBBmζ CAR T cells assessed by MFI of MitoGreen staining.

758

759 **Supplemental Fig. 3: Short duration of CD28 blockade does not impair early anti-tumor**  
760 **responses but may reduce systemic toxicities by dampening pro-inflammatory cytokines**  
761 **in the BM, related to figure 4 and figure 5.**

- 762 **(A)** Flow cytometry gating strategy used to determine tumor burden and CAR T cell frequency  
763 following BM harvest of 5TGM1 bearing RAG2<sup>-/-</sup> mice treated with CD28<sup>fl/fl</sup> mBBmζ CAR T  
764 cells ± abatacept for 7 days.

- 765 **(B)** Tumor burden assessed by the frequency of mCD138<sup>+</sup> B220<sup>-</sup> cells in the BM of 5TGM1  
766 bearing RAG2<sup>-/-</sup> mice treated with CD28<sup>fl/fl</sup> mBBmζ CAR T cells ± abatacept for 7 days. Each  
767 data point represents an individual tumor bearing host. Significance determined by one-way  
768 ANOVA.



769 **Supplemental Table Captions:**

770 1. Mouse and human antibodies used for cell phenotyping analyses performed by flow  
771 cytometry.

772 2. Mouse primer sequences used for qRT-PCR.

773

774

## 775 References

776

- 777 1 Cappell, K. M. & Kochenderfer, J. N. Long-term outcomes following CAR T cell therapy: what we  
778 know so far. *Nat Rev Clin Oncol* **20**, 359-371, doi:10.1038/s41571-023-00754-1 (2023).
- 779 2 Cappell, K. M. *et al.* Long-Term Follow-Up of Anti-CD19 Chimeric Antigen Receptor T-Cell  
780 Therapy. *J Clin Oncol* **38**, 3805-3815, doi:10.1200/jco.20.01467 (2020).
- 781 3 Kochenderfer, J. N. *et al.* B-cell depletion and remissions of malignancy along with cytokine-  
782 associated toxicity in a clinical trial of anti-CD19 chimeric-antigen-receptor-transduced T cells.  
783 *Blood* **119**, 2709-2720, doi:10.1182/blood-2011-10-384388 (2012).
- 784 4 Kochenderfer, J. N. *et al.* Eradication of B-lineage cells and regression of lymphoma in a patient  
785 treated with autologous T cells genetically engineered to recognize CD19. *Blood* **116**, 4099-4102,  
786 doi:10.1182/blood-2010-04-281931 (2010).
- 787 5 Kalos, M. *et al.* T cells with chimeric antigen receptors have potent antitumor effects and can  
788 establish memory in patients with advanced leukemia. *Sci Transl Med* **3**, 95ra73,  
789 doi:10.1126/scitranslmed.3002842 (2011).
- 790 6 Maude, S. L. *et al.* Chimeric antigen receptor T cells for sustained remissions in leukemia. *N Engl J*  
791 *Med* **371**, 1507-1517, doi:10.1056/NEJMoa1407222 (2014).
- 792 7 Melenhorst, J. J. *et al.* Decade-long leukaemia remissions with persistence of CD4+ CAR T cells.  
793 *Nature* **602**, 503-509, doi:10.1038/s41586-021-04390-6 (2022).
- 794 8 Porter, D. L. *et al.* Chimeric antigen receptor T cells persist and induce sustained remissions in  
795 relapsed refractory chronic lymphocytic leukemia. *Sci Transl Med* **7**, 303ra139,  
796 doi:10.1126/scitranslmed.aac5415 (2015).
- 797 9 Porter, D. L., Levine, B. L., Kalos, M., Bagg, A. & June, C. H. Chimeric antigen receptor-modified T  
798 cells in chronic lymphoid leukemia. *N Engl J Med* **365**, 725-733, doi:10.1056/NEJMoa1103849  
799 (2011).
- 800 10 Neelapu, S. S. *et al.* Axicabtagene Ciloleucel CAR T-Cell Therapy in Refractory Large B-Cell  
801 Lymphoma. *N Engl J Med* **377**, 2531-2544, doi:10.1056/NEJMoa1707447 (2017).
- 802 11 Locke, F. L. *et al.* Long-term safety and activity of axicabtagene ciloleucel in refractory large B-cell  
803 lymphoma (ZUMA-1): a single-arm, multicentre, phase 1-2 trial. *Lancet Oncol* **20**, 31-42,  
804 doi:10.1016/s1470-2045(18)30864-7 (2019).
- 805 12 Locke, F. L. *et al.* Axicabtagene Ciloleucel as Second-Line Therapy for Large B-Cell Lymphoma. *N*  
806 *Engl J Med* **386**, 640-654, doi:10.1056/NEJMoa2116133 (2022).
- 807 13 Sadelain, M., Rivière, I. & Riddell, S. Therapeutic T cell engineering. *Nature* **545**, 423-431,  
808 doi:10.1038/nature22395 (2017).
- 809 14 Kochenderfer, J. N. & Rosenberg, S. A. Treating B-cell cancer with T cells expressing anti-CD19  
810 chimeric antigen receptors. *Nat Rev Clin Oncol* **10**, 267-276, doi:10.1038/nrclinonc.2013.46  
811 (2013).
- 812 15 June, C. H. & Sadelain, M. Chimeric Antigen Receptor Therapy. *N Engl J Med* **379**, 64-73,  
813 doi:10.1056/NEJMra1706169 (2018).
- 814 16 Cappell, K. M. & Kochenderfer, J. N. A comparison of chimeric antigen receptors containing CD28  
815 versus 4-1BB costimulatory domains. *Nature Reviews Clinical Oncology* **18**, 715-727,  
816 doi:10.1038/s41571-021-00530-z (2021).
- 817 17 Honikel, M. M. & Olejniczak, S. H. Co-Stimulatory Receptor Signaling in CAR-T Cells. *Biomolecules*  
818 **12**, doi:10.3390/biom12091303 (2022).
- 819 18 Guedan, S. *et al.* ICOS-based chimeric antigen receptors program bipolar TH17/TH1 cells. *Blood*  
820 **124**, 1070-1080, doi:10.1182/blood-2013-10-535245 (2014).
- 821 19 Guedan, S. *et al.* Enhancing CAR T cell persistence through ICOS and 4-1BB costimulation. *JCI*  
822 *Insight* **3**, doi:10.1172/jci.insight.96976 (2018).

- 823 20 Tan, J. *et al.* Chimeric antigen receptors containing the OX40 signalling domain enhance the  
824 persistence of T cells even under repeated stimulation with multiple myeloma target cells.  
825 *Journal of Hematology & Oncology* **15**, 39, doi:10.1186/s13045-022-01244-0 (2022).
- 826 21 Zhang, H. *et al.* A chimeric antigen receptor with antigen-independent OX40 signaling mediates  
827 potent antitumor activity. *Sci Transl Med* **13**, doi:10.1126/scitranslmed.aba7308 (2021).
- 828 22 Abramson, J. S. *et al.* Lisocabtagene maraleucel for patients with relapsed or refractory large B-  
829 cell lymphomas (TRANSCEND NHL 001): a multicentre seamless design study. *Lancet* **396**, 839-  
830 852, doi:10.1016/s0140-6736(20)31366-0 (2020).
- 831 23 Schuster, S. J. *et al.* Tisagenlecleucel in Adult Relapsed or Refractory Diffuse Large B-Cell  
832 Lymphoma. *N Engl J Med* **380**, 45-56, doi:10.1056/NEJMoa1804980 (2019).
- 833 24 Shah, B. D. *et al.* KTE-X19 for relapsed or refractory adult B-cell acute lymphoblastic leukaemia:  
834 phase 2 results of the single-arm, open-label, multicentre ZUMA-3 study. *Lancet* **398**, 491-502,  
835 doi:10.1016/s0140-6736(21)01222-8 (2021).
- 836 25 Munshi, N. C. *et al.* Idecabtagene vicleucel in Relapsed and Refractory Multiple Myeloma. *New*  
837 *England Journal of Medicine* **384**, 705-716, doi:10.1056/nejmoa2024850 (2021).
- 838 26 Berdeja, J. G. *et al.* Ciltacabtagene autoleucel, a B-cell maturation antigen-directed chimeric  
839 antigen receptor T-cell therapy in patients with relapsed or refractory multiple myeloma  
840 (CARTITUDE-1): a phase 1b/2 open-label study. *Lancet* **398**, 314-324, doi:10.1016/s0140-  
841 6736(21)00933-8 (2021).
- 842 27 San-Miguel, J. *et al.* Cilta-cel or Standard Care in Lenalidomide-Refractory Multiple Myeloma.  
843 *New England Journal of Medicine* **389**, 335-347, doi:10.1056/NEJMoa2303379 (2023).
- 844 28 Rejeski, K., Jain, M. D. & Smith, E. L. Mechanisms of Resistance and Treatment of Relapse after  
845 CAR T-cell Therapy for Large B-cell Lymphoma and Multiple Myeloma. *Transplant Cell Ther* **29**,  
846 418-428, doi:10.1016/j.jtct.2023.04.007 (2023).
- 847 29 Rodriguez-Otero, P. *et al.* Ide-cel or Standard Regimens in Relapsed and Refractory Multiple  
848 Myeloma. *New England Journal of Medicine* **388**, 1002-1014, doi:10.1056/NEJMoa2213614  
849 (2023).
- 850 30 Lightman, S. M., Utley, A. & Lee, K. P. Survival of Long-Lived Plasma Cells (LLPC): Piecing Together  
851 the Puzzle. *Frontiers in Immunology* **10**, doi:10.3389/fimmu.2019.00965 (2019).
- 852 31 Aggarwal, R., Ghobrial, I. M. & Roodman, G. D. Chemokines in multiple myeloma. *Exp Hematol*  
853 **34**, 1289-1295, doi:10.1016/j.exphem.2006.06.017 (2006).
- 854 32 Alsayed, Y. *et al.* Mechanisms of regulation of CXCR4/SDF-1 (CXCL12)-dependent migration and  
855 homing in multiple myeloma. *Blood* **109**, 2708-2717, doi:10.1182/blood-2006-07-035857 (2007).
- 856 33 Ahsmann, E. J., Lokhorst, H. M., Dekker, A. W. & Bloem, A. C. Lymphocyte function-associated  
857 antigen-1 expression on plasma cells correlates with tumor growth in multiple myeloma. *Blood*  
858 **79**, 2068-2075 (1992).
- 859 34 Moser-Katz, T., Joseph, N. S., Dhodapkar, M. V., Lee, K. P. & Boise, L. H. Game of Bones: How  
860 Myeloma Manipulates Its Microenvironment. *Frontiers in Oncology* **10**,  
861 doi:10.3389/fonc.2020.625199 (2021).
- 862 35 Tai, Y. T. *et al.* APRIL and BCMA promote human multiple myeloma growth and  
863 immunosuppression in the bone marrow microenvironment. *Blood* **127**, 3225-3236,  
864 doi:10.1182/blood-2016-01-691162 (2016).
- 865 36 Moreaux, J. *et al.* BAFF and APRIL protect myeloma cells from apoptosis induced by interleukin 6  
866 deprivation and dexamethasone. *Blood* **103**, 3148-3157, doi:10.1182/blood-2003-06-1984  
867 (2004).
- 868 37 Novak, A. J. *et al.* Expression of BCMA, TACI, and BAFF-R in multiple myeloma: a mechanism for  
869 growth and survival. *Blood* **103**, 689-694, doi:10.1182/blood-2003-06-2043 (2004).

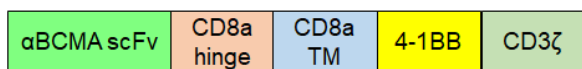
- 870 38 Chauhan, D. *et al.* Multiple myeloma cell adhesion-induced interleukin-6 expression in bone  
871 marrow stromal cells involves activation of NF-kappa B. *Blood* **87**, 1104-1112 (1996).
- 872 39 Uchiyama, H., Barut, B. A., Mohrbacher, A. F., Chauhan, D. & Anderson, K. C. Adhesion of human  
873 myeloma-derived cell lines to bone marrow stromal cells stimulates interleukin-6 secretion.  
874 *Blood* **82**, 3712-3720 (1993).
- 875 40 Hideshima, T., Nakamura, N., Chauhan, D. & Anderson, K. C. Biologic sequelae of interleukin-6  
876 induced PI3-K/Akt signaling in multiple myeloma. *Oncogene* **20**, 5991-6000,  
877 doi:10.1038/sj.onc.1204833 (2001).
- 878 41 Robillard, N. *et al.* CD28, a marker associated with tumoral expansion in multiple myeloma. *Clin*  
879 *Cancer Res* **4**, 1521-1526 (1998).
- 880 42 Gavile, C. M. *et al.* CD86 regulates myeloma cell survival. *Blood Adv* **1**, 2307-2319,  
881 doi:10.1182/bloodadvances.2017011601 (2017).
- 882 43 Koorella, C. *et al.* Novel regulation of CD80/CD86-induced phosphatidylinositol 3-kinase signaling  
883 by NOTCH1 protein in interleukin-6 and indoleamine 2,3-dioxygenase production by dendritic  
884 cells. *J Biol Chem* **289**, 7747-7762, doi:10.1074/jbc.M113.519686 (2014).
- 885 44 Lightman, S. M. *et al.* Indoleamine 2,3-dioxygenase 1 is essential for sustaining durable antibody  
886 responses. *Immunity* **54**, 2772-2783.e2775, doi:<https://doi.org/10.1016/j.immuni.2021.10.005>  
887 (2021).
- 888 45 Murray, M. E. *et al.* CD28-mediated pro-survival signaling induces chemotherapeutic resistance  
889 in multiple myeloma. *Blood* **123**, 3770-3779, doi:10.1182/blood-2013-10-530964 (2014).
- 890 46 Bahlis, N. J. *et al.* CD28-mediated regulation of multiple myeloma cell proliferation and survival.  
891 *Blood* **109**, 5002-5010, doi:10.1182/blood-2006-03-012542 (2007).
- 892 47 Utley, A. *et al.* CD28 Regulates Metabolic Fitness for Long-Lived Plasma Cell Survival. *Cell Rep* **31**,  
893 107815, doi:10.1016/j.celrep.2020.107815 (2020).
- 894 48 Rubbert-Roth, A. *et al.* Trial of Upadacitinib or Abatacept in Rheumatoid Arthritis. *N Engl J Med*  
895 **383**, 1511-1521, doi:10.1056/NEJMoa2008250 (2020).
- 896 49 Watkins, B. *et al.* Phase II Trial of Costimulation Blockade With Abatacept for Prevention of Acute  
897 GVHD. *J Clin Oncol* **39**, 1865-1877, doi:10.1200/jco.20.01086 (2021).
- 898 50 Shalaby, K. *et al.* Phase 2 study of abatacept, ixazomib, and dexamethasone in patients with  
899 relapsed/refractory multiple myeloma. *Journal of Clinical Oncology* **41**, 8030-8030,  
900 doi:10.1200/JCO.2023.41.16\_suppl.8030 (2023).
- 901 51 Salter, A. I. *et al.* Phosphoproteomic analysis of chimeric antigen receptor signaling reveals  
902 kinetic and quantitative differences that affect cell function. *Science Signaling* **11**, eaat6753,  
903 doi:10.1126/scisignal.aat6753 (2018).
- 904 52 Feucht, J. & Sadelain, M. Function and evolution of the prototypic CD28 $\zeta$  and 4-1BB $\zeta$  chimeric  
905 antigen receptors. *Immuno-oncol Technol* **8**, 2-11, doi:10.1016/j.iotech.2020.09.001 (2020).
- 906 53 Long, A. H. *et al.* 4-1BB costimulation ameliorates T cell exhaustion induced by tonic signaling of  
907 chimeric antigen receptors. *Nat Med* **21**, 581-590, doi:10.1038/nm.3838 (2015).
- 908 54 Kawalekar, O. U. *et al.* Distinct Signaling of Coreceptors Regulates Specific Metabolism Pathways  
909 and Impacts Memory Development in CAR T Cells. *Immunity* **44**, 380-390,  
910 doi:10.1016/j.immuni.2016.01.021 (2016).
- 911 55 Agarwal, S. *et al.* Deletion of the inhibitory co-receptor CTLA-4 enhances and invigorates  
912 chimeric antigen receptor T cells. *Immunity* **56**, 2388-2407.e2389,  
913 doi:10.1016/j.immuni.2023.09.001 (2023).
- 914 56 Prokhnevskaya, N. *et al.* CD8(+) T cell activation in cancer comprises an initial activation phase in  
915 lymph nodes followed by effector differentiation within the tumor. *Immunity* **56**, 107-124 e105,  
916 doi:10.1016/j.immuni.2022.12.002 (2023).

- 917 57 Smith, E. L. *et al.* Development and Evaluation of an Optimal Human Single-Chain Variable  
918 Fragment-Derived BCMA-Targeted CAR T Cell Vector. *Mol Ther* **26**, 1447-1456,  
919 doi:10.1016/j.ymthe.2018.03.016 (2018).
- 920 58 Li, G. *et al.* 4-1BB enhancement of CAR T function requires NF- $\kappa$ B and TRAFs. *JCI Insight* **3**,  
921 doi:10.1172/jci.insight.121322 (2018).
- 922 59 Works, M. *et al.* Anti-B-cell Maturation Antigen Chimeric Antigen Receptor T cell Function  
923 against Multiple Myeloma Is Enhanced in the Presence of Lenalidomide. *Mol Cancer Ther* **18**,  
924 2246-2257, doi:10.1158/1535-7163.Mct-18-1146 (2019).
- 925 60 Hammill, J. A., Afsahi, A., Bramson, J. L. & Helsen, C. W. Viral Engineering of Chimeric Antigen  
926 Receptor Expression on Murine and Human T Lymphocytes. *Methods Mol Biol* **1458**, 137-157,  
927 doi:10.1007/978-1-4939-3801-8\_11 (2016).
- 928 61 Chu, V. T. *et al.* Efficient generation of Rosa26 knock-in mice using CRISPR/Cas9 in C57BL/6  
929 zygotes. *BMC Biotechnology* **16**, 4, doi:10.1186/s12896-016-0234-4 (2016).
- 930 62 Fowler, J. A., Mundy, G. R., Lwin, S. T., Lynch, C. C. & Edwards, C. M. A murine model of myeloma  
931 that allows genetic manipulation of the host microenvironment. *Dis Model Mech* **2**, 604-611,  
932 doi:10.1242/dmm.003160 (2009).
- 933 63 Dallas, S. L. *et al.* Ibandronate reduces osteolytic lesions but not tumor burden in a murine  
934 model of myeloma bone disease. *Blood* **93**, 1697-1706 (1999).
- 935 64 Radl, J., De Glopper, E. D., Schuit, H. R. & Zurcher, C. Idiopathic paraproteinemia. II.  
936 Transplantation of the paraprotein-producing clone from old to young C57BL/KaLwRij mice. *J*  
937 *Immunol* **122**, 609-613 (1979).
- 938 65 Asosingh, K., Radl, J., Van Riet, I., Van Camp, B. & Vanderkerken, K. The 5TMM series: a useful in  
939 vivo mouse model of human multiple myeloma. *Hematol J* **1**, 351-356,  
940 doi:10.1038/sj.thj.6200052 (2000).
- 941 66 Frauwirth, K. A. *et al.* The CD28 signaling pathway regulates glucose metabolism. *Immunity* **16**,  
942 769-777, doi:10.1016/s1074-7613(02)00323-0 (2002).
- 943 67 Klein Geltink, R. I. *et al.* Mitochondrial Priming by CD28. *Cell* **171**, 385-397.e311,  
944 doi:10.1016/j.cell.2017.08.018 (2017).
- 945 68 Beckermann, K. E. *et al.* CD28 costimulation drives tumor-infiltrating T cell glycolysis to promote  
946 inflammation. *JCI Insight* **5**, doi:10.1172/jci.insight.138729 (2020).
- 947 69 Holling, G. A. *et al.* CD8+ T cell metabolic flexibility elicited by CD28-ARS2 axis-driven alternative  
948 splicing of PKM supports antitumor immunity. *Cell Mol Immunol*, doi:10.1038/s41423-024-  
949 01124-2 (2024).
- 950 70 Nanjireddy, P. M., Olejniczak, S. H. & Buxbaum, N. P. Targeting of chimeric antigen receptor T cell  
951 metabolism to improve therapeutic outcomes. *Front Immunol* **14**, 1121565,  
952 doi:10.3389/fimmu.2023.1121565 (2023).
- 953 71 Birsoy, K. *et al.* An Essential Role of the Mitochondrial Electron Transport Chain in Cell  
954 Proliferation Is to Enable Aspartate Synthesis. *Cell* **162**, 540-551, doi:10.1016/j.cell.2015.07.016  
955 (2015).
- 956 72 Sullivan, L. B. *et al.* Supporting Aspartate Biosynthesis Is an Essential Function of Respiration in  
957 Proliferating Cells. *Cell* **162**, 552-563, doi:10.1016/j.cell.2015.07.017 (2015).
- 958 73 Chewing, J. H., Dugger, K. J., Chaudhuri, T. R., Zinn, K. R. & Weaver, C. T. Bioluminescence-based  
959 visualization of CD4 T cell dynamics using a T lineage-specific luciferase transgenic model. *BMC*  
960 *Immunol* **10**, 44, doi:10.1186/1471-2172-10-44 (2009).
- 961 74 Torvinen, M., Campwala, H. & Kilty, I. The role of IFN- $\gamma$  in regulation of IFN- $\gamma$ -inducible protein 10  
962 (IP-10) expression in lung epithelial cell and peripheral blood mononuclear cell co-cultures.  
963 *Respiratory Research* **8**, 80, doi:10.1186/1465-9921-8-80 (2007).

- 964 75 Trinchieri, G. Interleukin-12 and the regulation of innate resistance and adaptive immunity.  
965 *Nature Reviews Immunology* **3**, 133-146, doi:10.1038/nri1001 (2003).
- 966 76 Rejeski, K. *et al.* Immune effector cell-associated hematotoxicity: EHA/EBMT consensus grading  
967 and best practice recommendations. *Blood* **142**, 865-877, doi:10.1182/blood.2023020578  
968 (2023).
- 969 77 Shimabukuro-Vornhagen, A. *et al.* Cytokine release syndrome. *Journal for immunotherapy of*  
970 *cancer* **6**, 1-14 (2018).
- 971 78 Karschnia, P. *et al.* Clinical presentation, management, and biomarkers of neurotoxicity after  
972 adoptive immunotherapy with CAR T cells. *Blood, The Journal of the American Society of*  
973 *Hematology* **133**, 2212-2221 (2019).
- 974 79 Haseeb, F., Tholouli, E. & Wilson, A. Chimeric antigen receptor T-cell therapy in adults:  
975 management of toxicities and implications for critical care. *BJA Educ* **22**, 330-333,  
976 doi:10.1016/j.bjae.2022.04.001 (2022).
- 977 80 Strati, P. *et al.* Clinical efficacy of anakinra to mitigate CAR T-cell therapy-associated toxicity in  
978 large B-cell lymphoma. *Blood Advances* **4**, 3123-3127, doi:10.1182/bloodadvances.2020002328  
979 (2020).
- 980 81 Ngwube, A., Rangarajan, H. & Shah, N. Role of abatacept in the prevention of graft-versus-host  
981 disease: current perspectives. *Therapeutic Advances in Hematology* **14**, 20406207231152644,  
982 doi:10.1177/20406207231152644 (2023).
- 983 82 Blair, H. A. & Deeks, E. D. Abatacept: A Review in Rheumatoid Arthritis. *Drugs* **77**, 1221-1233,  
984 doi:10.1007/s40265-017-0775-4 (2017).
- 985 83 Brentjens, R. J. *et al.* Eradication of systemic B-cell tumors by genetically targeted human T  
986 lymphocytes co-stimulated by CD80 and interleukin-15. *Nature Medicine* **9**, 279-286,  
987 doi:10.1038/nm827 (2003).
- 988 84 Brentjens, R. J. *et al.* Genetically Targeted T Cells Eradicate Systemic Acute Lymphoblastic  
989 Leukemia Xenografts. *Clinical Cancer Research* **13**, 5426-5435, doi:10.1158/1078-0432.Ccr-07-  
990 0674 (2007).
- 991 85 Boucher, J. C. *et al.* CD28 Costimulatory Domain-Targeted Mutations Enhance Chimeric Antigen  
992 Receptor T-cell Function. *Cancer Immunology Research* **9**, 62-74, doi:10.1158/2326-6066.cir-20-  
993 0253 (2021).
- 994 86 Guedan, S. *et al.* Single residue in CD28-costimulated CAR-T cells limits long-term persistence  
995 and antitumor durability. *J Clin Invest* **130**, 3087-3097, doi:10.1172/jci133215 (2020).
- 996 87 Wijewarnasuriya, D., Beberitz, C., Lopez, A. V., Rafiq, S. & Brentjens, R. J. Excessive  
997 Costimulation Leads to Dysfunction of Adoptively Transferred T Cells. *Cancer Immunol Res* **8**,  
998 732-742, doi:10.1158/2326-6066.Cir-19-0908 (2020).
- 999 88 Duraiswamy, J. *et al.* Myeloid antigen-presenting cell niches sustain antitumor T cells and license  
1000 PD-1 blockade via CD28 costimulation. *Cancer Cell* **39**, 1623-1642 e1620,  
1001 doi:10.1016/j.ccell.2021.10.008 (2021).
- 1002 89 Pope, B., Brown, R. D., Gibson, J., Yuen, E. & Joshua, D. B7-2-positive myeloma: incidence, clinical  
1003 characteristics, prognostic significance, and implications for tumor immunotherapy. *Blood* **96**,  
1004 1274-1279 (2000).
- 1005 90 Chaperot, L. *et al.* Functional expression of CD80 and CD86 allows immunogenicity of malignant  
1006 B cells from non-Hodgkin's lymphomas. *Experimental Hematology* **27**, 479-488,  
1007 doi:[https://doi.org/10.1016/S0301-472X\(98\)00059-9](https://doi.org/10.1016/S0301-472X(98)00059-9) (1999).
- 1008 91 Sędek, Ł. *et al.* Differential expression of CD73, CD86 and CD304 in normal vs. leukemic B-cell  
1009 precursors and their utility as stable minimal residual disease markers in childhood B-cell  
1010 precursor acute lymphoblastic leukemia. *Journal of Immunological Methods* **475**, 112429,  
1011 doi:<https://doi.org/10.1016/j.jim.2018.03.005> (2019).

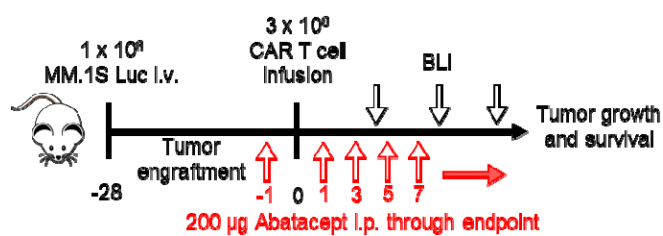


A.

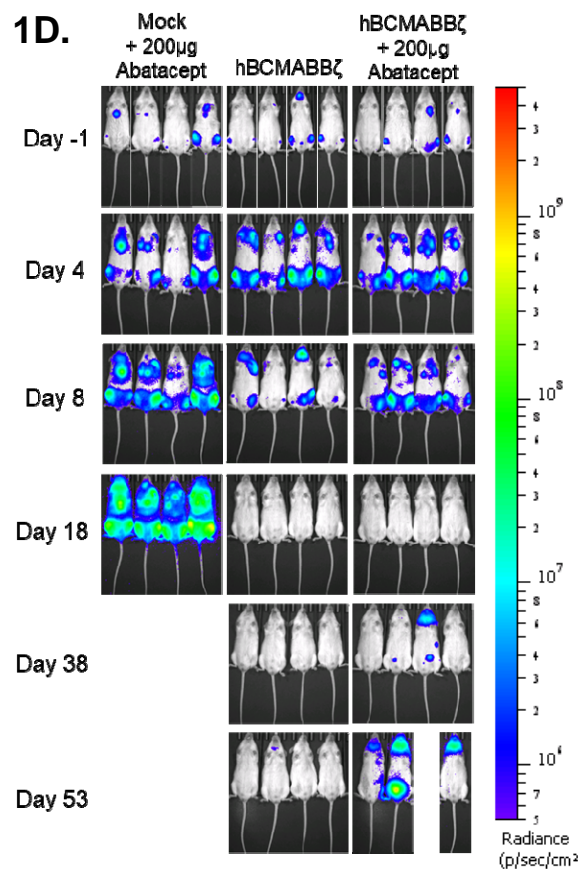


B.

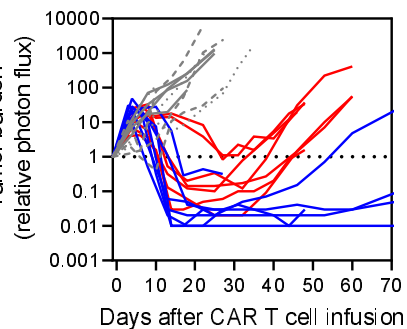
C.



D.



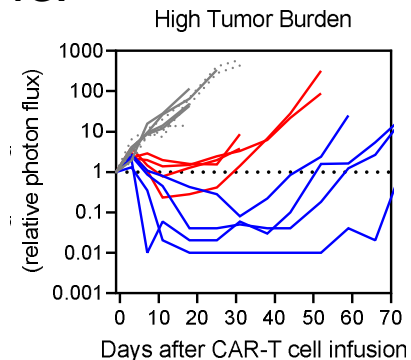
E.



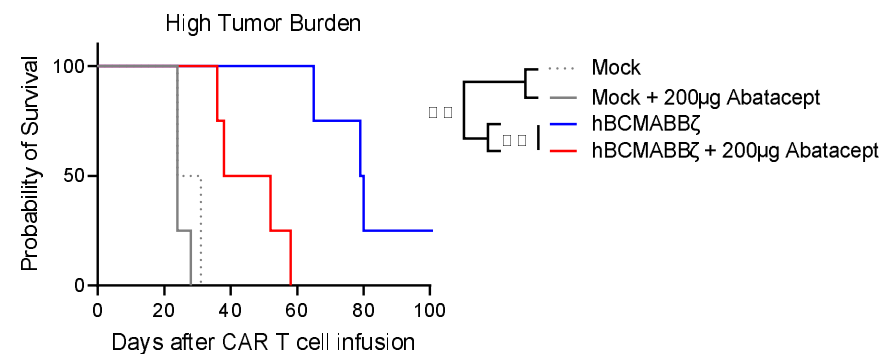
F.



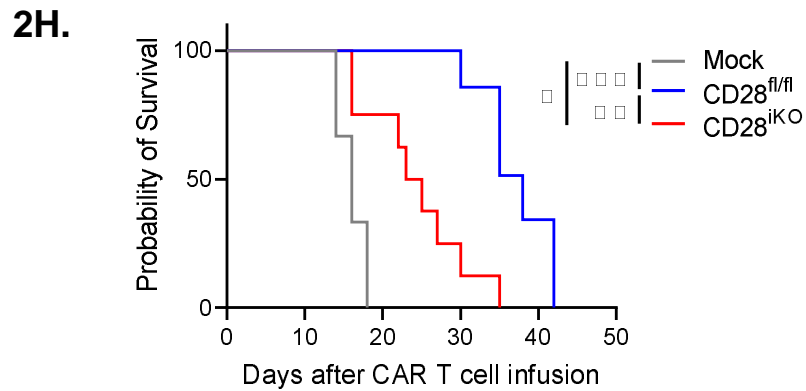
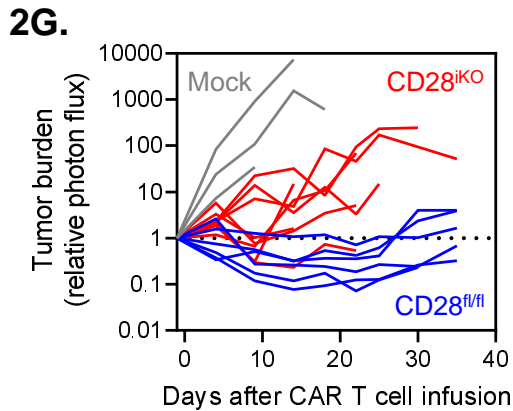
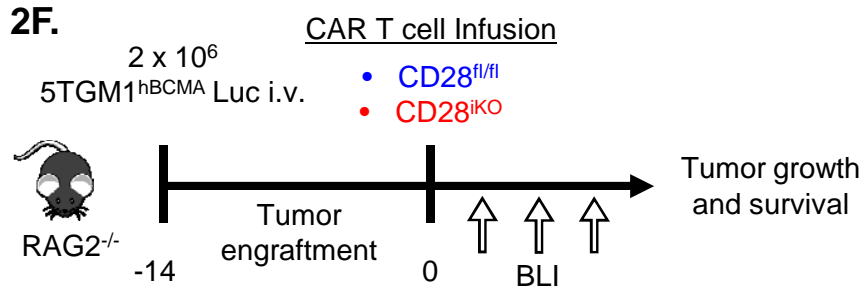
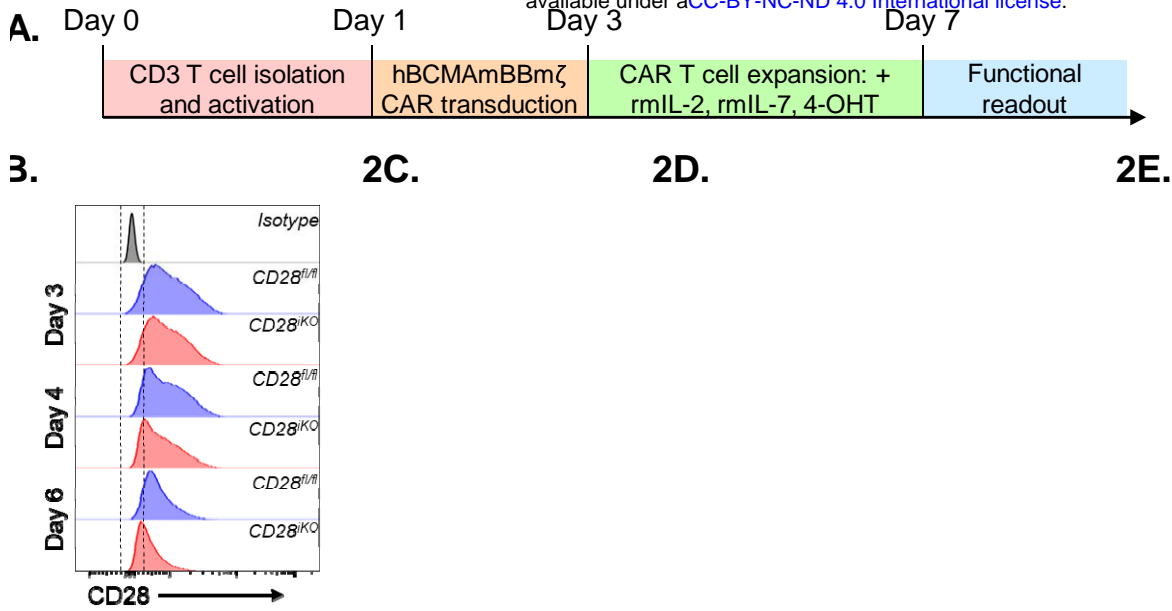
G.



H.







**2I.**

3A.

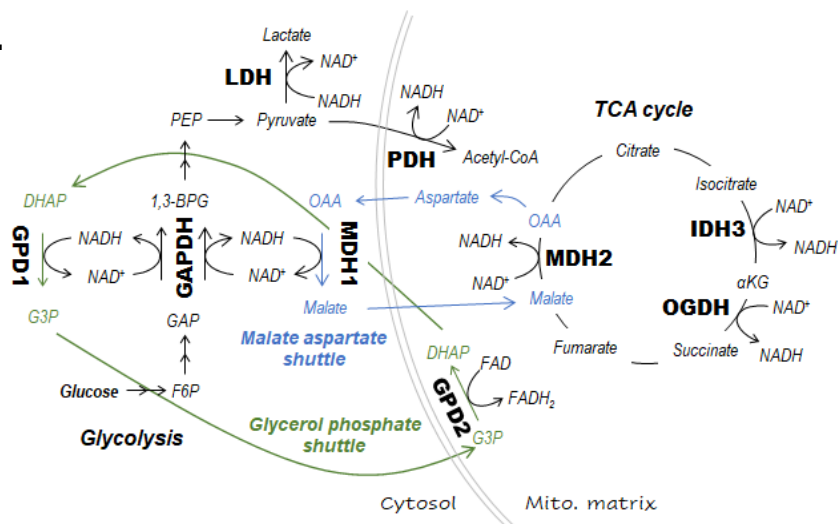
3B.

3C.

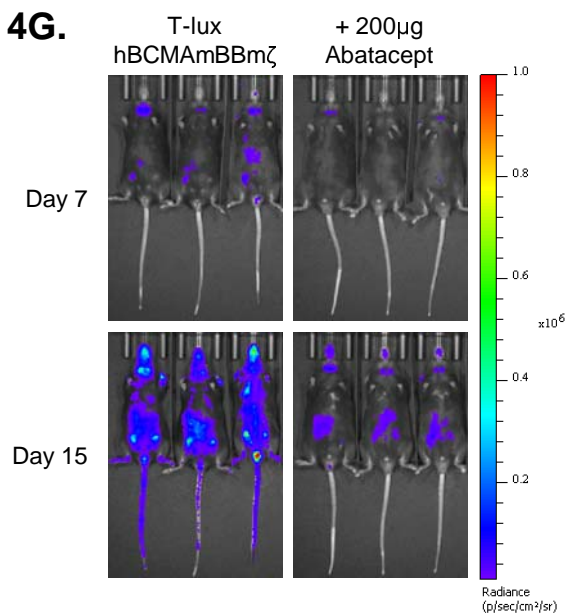
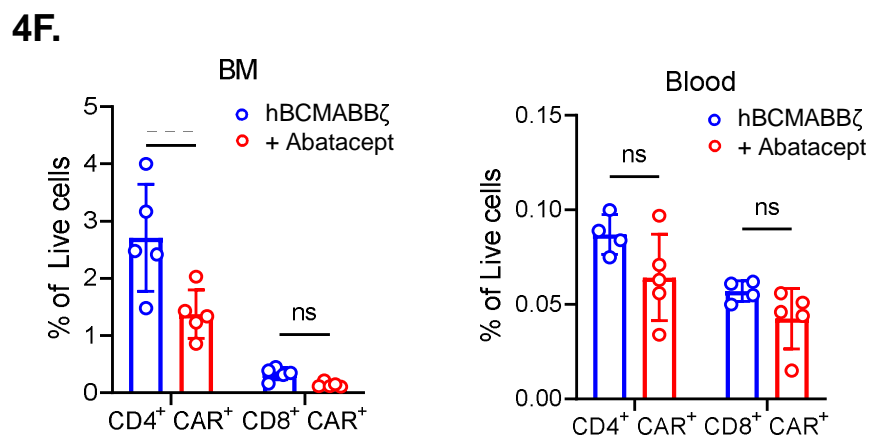
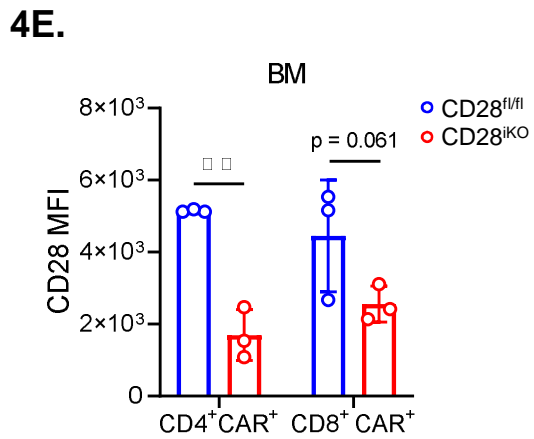
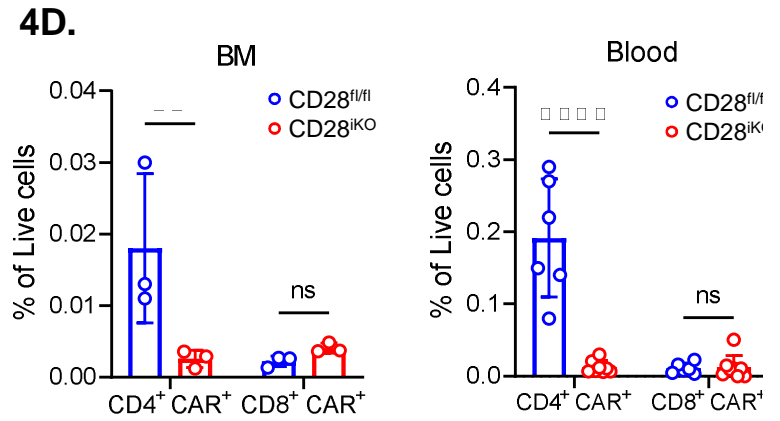
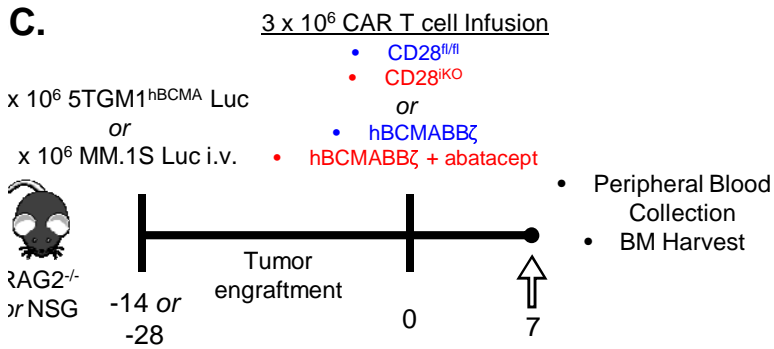
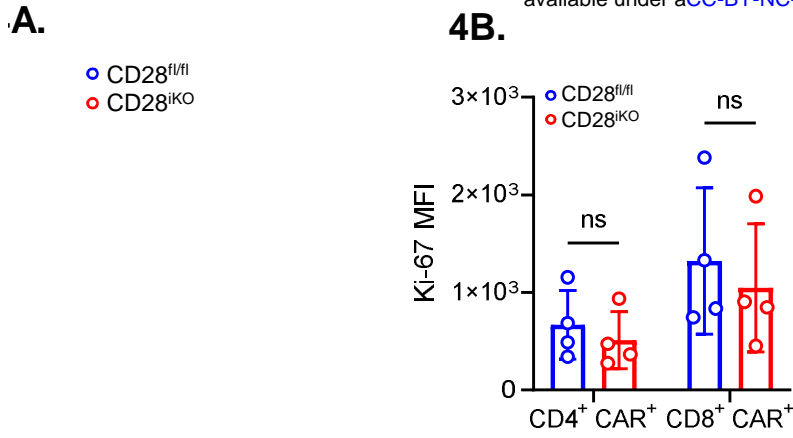
3D.

3E.

3F.

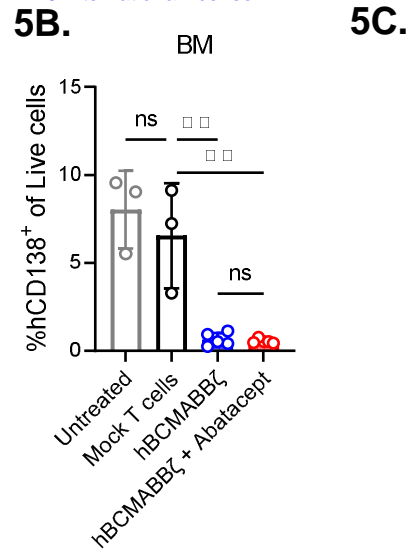
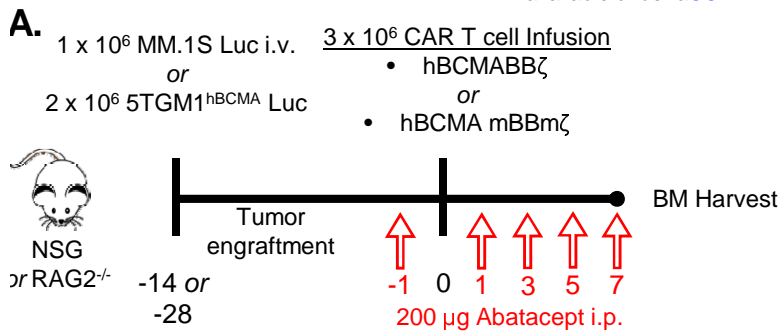


3G.



**4H.**

## Figure 5



5D.

5E.

